

2023

# Defining the role of SMARCAL1 at alternatively-lengthened telomeres

---

<https://hdl.handle.net/2144/47453>

*Downloaded from DSpace Repository, DSpace Institution's institutional repository*

BOSTON UNIVERSITY

ARAM V. CHOBANIAN & EDWARD AVEDISIAN SCHOOL OF MEDICINE

Dissertation

**DEFINING THE ROLE OF SMARCA1  
AT ALTERNATIVELY-LENGTHENED TELOMERES**

by

**LISA CARSON**

A.B., Dartmouth College, 2015

Submitted in partial fulfillment of the

requirements for the degree of

Doctor of Philosophy

2023

© 2023 by  
LISA CARSON  
All rights reserved

Approved by

First Reader

---

Rachel Litman Flynn, Ph.D.  
Associate Professor of Pharmacology and Medicine

Second Reader

---

Christopher Heaphy, Ph.D.  
Assistant Professor of Medicine and Pathology & Laboratory Medicine

## **DEDICATION**

I dedicate this work to my parents, Janet and Steve Carson, for their constant love and support.

## ACKNOWLEDGMENTS

I want to begin this dissertation by acknowledging some of the many people who made it possible. To begin with, I want to thank Dr. Rachel Flynn for many years of patience and encouragement. Rachel, thank you for not firing me even when I specifically asked you to. Even when nothing was working at all, you could always rope me back in. Your genuine scientific curiosity is deranged but inspirational.

I also need to thank the members of my dissertation advisory committee, who could have verbally eviscerated me on many occasions but chose not to. Dr. Gerald Denis, thank you for chairing my committee and for taking an interest in my life outside of the lab. Dr. Andy Henderson, I appreciate that you were willing to be on my committee somewhat randomly, but always had incredibly helpful questions and insights. Dr. Chris Heaphy, thank you for bringing your vast amount of ALT-related knowledge to the table. And Dr. Hui Feng, I appreciated having you around on K7 to discuss science and to race to work every morning. Additionally, I would like to thank Dr. Matt Jones and everyone else involved in the Program in Molecular and Translational Medicine.

To my K7 friends and coworkers: you are all incredible people and scientists, and I cannot wait to see the amazing things you will do. Thank you for making this slightly more tolerable. Finally, I would like to acknowledge all my friends and family members who have had to put up with me over the past five years, especially my parents and my husband, Jonathan Griffith. Thank you for your patience and support, and for everything else you have all done for me over the years.

**DEFINING THE ROLE OF SMARCAL1  
AT ALTERNATIVELY-LENGTHENED TELOMERES**

**LISA CARSON**

Boston University Aram V. Chobanian & Edward Avedisian School of Medicine, 2023

Major Professor: Rachel Litman Flynn, Ph.D., Associate Professor of Pharmacology and  
Medicine

**ABSTRACT**

Cellular immortalization is a prerequisite of cancers and depends upon evasion of telomeric erosion that would otherwise lead to replicative senescence. A subset of cancers achieves telomere maintenance via a pathway known as Alternative Lengthening of Telomeres (ALT), which relies on homologous recombination that is driven by chronic DNA replication stress and allows for telomeric elongation events. Here, we sought to further elucidate the role of the annealing helicase SMARCAL1, which reverses and stabilizes stalled replication forks, in cancers that utilize ALT. SMARCAL1 is crucial to resolve the replication stress at ALT telomeres, but paradoxically is lost in a subset of ALT-positive tumors. Other common ALT-related mutations occur in the ATRX/DAXX complex, which deposits the histone variant H3.3 at telomeres. In contrast to loss of ATRX, we found that SMARCAL1 depletion does not affect H3.3 deposition, but does lead to changes in trimethylation of histone 3 lysine 9 that may create an ALT-permissive state. We also found that ALT-positive cell lines are more sensitive to combined depletion of SMARCAL1 and ATRX. Furthermore, we discovered that SMARCAL1 interacts with heterochromatin protein 1 (HP1), and that loss of SMARCAL1 deregulates

the presence of HP1 at telomeres, providing a link to changes in histone methylation. We also identified a novel complex between SMARCAL1, HP1, and the histone methyltransferase SETDB1. Overall, our results indicate that SMARCAL1 is an important factor in telomeric chromatin formation, indicating a previously undescribed role for SMARCAL1 in genome maintenance.

## TABLE OF CONTENTS

DEDICATION .....	iv
ACKNOWLEDGMENTS .....	v
ABSTRACT .....	vi
TABLE OF CONTENTS.....	viii
LIST OF TABLES .....	xii
LIST OF FIGURES .....	xiii
LIST OF ABBREVIATIONS.....	xiv
CHAPTER ONE: INTRODUCTION.....	1
Telomere Structure and Function .....	1
Telomere Maintenance .....	3
Telomerase.....	6
Alternative Lengthening of Telomeres .....	6
Ever-Shorter Telomeres .....	9
Telomeric DNA Damage and Replication Stress .....	9
Telomeric Replication Stress .....	9
ALT Replication Stress.....	10
Hallmarks of ALT.....	12
Genetics of ALT .....	14
ATRX/DAXX.....	14
SLX4IP & TOP3A.....	15
SMARCAL1 .....	15

SMARCAL1 and ALT.....	16
Concluding Remarks.....	18
Hypothesis and Aims .....	18
CHAPTER TWO: SMARCAL1 CONTRIBUTES TO TELOMERIC	
HETEROCHROMATIN MAINTENANCE .....	
Abstract.....	20
Introduction.....	20
Materials and Methods.....	22
Cell Lines and Culture Conditions.....	22
siRNA Transfection .....	23
Plasmid Overexpression.....	24
Lentiviral Infection/shRNA-Mediated Knockdown .....	25
Western Blots.....	25
Luminescence-Based Viability Assay .....	26
Immunofluorescence-Fluorescence in situ Hybridization (IF-FISH).....	27
Chromatin Immunoprecipitation (ChIP).....	28
Statistical Analysis.....	30
Results.....	30
SMARCAL1 loss does not affect ATRX localization to telomeres or H3.3	
deposition.....	30
SMARCAL1 loss changes H3K9 trimethylation at telomeres .....	34
ALT cells are sensitive to depletion of ATRX and SMARCAL1 .....	38

Discussion.....	41
CHAPTER THREE: SMARCAL1 INTERACTS WITH HETEROCHROMATIN	
MAINTENANCE MACHINERY .....	44
Abstract.....	44
Introduction.....	44
Materials & Methods .....	46
Cell Lines and Culture Conditions.....	46
siRNA Transfection .....	46
Lentiviral Infection/shRNA-Mediated Knockdown .....	47
Plasmid Overexpression.....	47
Western Blots.....	47
Luminescence-Based Viability Assay .....	48
Immunofluorescence-Fluorescence in situ Hybridization (IF-FISH).....	48
Chromatin Immunoprecipitation (ChIP).....	48
Immunoprecipitation (IP).....	49
Statistical Analysis.....	49
Results.....	50
SMARCAL1 interacts with heterochromatin protein 1 .....	50
HP1 does not recruit SMARCAL1 to telomeres.....	53
SMARCAL1 depletion changes HP1 localization to telomeres .....	56
SMARCAL1 forms a complex with SETDB1.....	60
Discussion.....	64

CHAPTER FOUR: FINAL THOUGHTS AND FUTURE DIRECTIONS .....	68
Summary .....	68
Future Directions .....	69
Final Thoughts .....	71
APPENDIX .....	72
REFERENCES .....	75
CURRICULUM VITAE.....	91

## LIST OF TABLES

Table 1. Major ALT-associated mutations .....	17
Table 2. Cell lines used.....	23

## LIST OF FIGURES

Figure 1: Telomeres are protected by shelterin-mediated T-loop formation.....	2
Figure 2: Schematic of the ALT mechanism. ....	8
Figure 3: SMARCAL1 loss does not displace ATRX from telomeres.....	32
Figure 4: SMARCAL1 depletion does not affect H3.3 incorporation at telomeres. ....	34
Figure 5: SMARCAL1 depletion leads to changes in H3K9me3.....	37
Figure 6: ALT cells are sensitive to combined depletion of SMARCAL1 and ATRX....	40
Figure 7: SMARCAL1 interacts with HP1 .....	51
Figure 8: SMARCAL1 mutants express poorly, but rescue viability in SaOS2.....	53
Figure 9: HP1 does not recruit SMARCAL1 to telomeres. ....	55
Figure 10: SMARCAL1 depletion changes HP1 isoform ratios at the telomere.....	58
Figure 11: SMARCAL1 and SETDB1 form a complex and may affect telomeric heterochromatin. ....	63
Figure 12: Hypothetical model demonstrating SMARCAL1 regulation of telomeric chromatin. ....	66
Supplementary figure: Western blots confirming knockdown .....	73

## LIST OF ABBREVIATIONS

53BP1	p53-binding protein 1
9-1-1	RAD9-RAD1-HUS1 complex
ALT	Alternative lengthening of telomeres
alt-NHEJ	Alternative non-homologous end joining
APB	ALT-associated PML body
ATM	Ataxia-telangiectasia mutated
ATR	ATM and Rad3-related
ATRIP	ATR-interacting protein
ATRX	$\alpha$ -thalassemia/mental retardation syndrome X-linked
BIR	Break-induced replication
BiTS	Break-induced telomere synthesis
BLM	Bloom's helicase
BSA	Bovine serum albumin
BTR	BLM-TOP3A-RMI complex
CD	Chromodomain
CDK1	Cyclin-dependent kinase 1
ChIP	Chromatin immunoprecipitation
CHK1	Checkpoint kinase 1
CHK2	Checkpoint kinase 2
c-NHEJ	Classical non-homologous end joining
CSD	Chromoshadow domain

CtIP	C-terminal binding protein interacting protein
DAPI	4',6-diamidino-2-phenylindole
DAXX	Death domain associated protein
DDR	DNA damage response
D-loop	Displacement loop
DMEM	Dulbecco's modified Eagle medium
DNA-PKcs	DNA-dependent protein kinase catalytic subunit
EMEM	Eagle's minimal essential medium
EST	Ever-shorter telomeres
FANCA	Fanconi anemia complementation group A
FANCD2	Fanconi anemia complementation group D2
FANCM	Fanconi anemia complementation group M
FBS	Fetal bovine serum
FEN1	Flap endonuclease 1
FISH	Fluorescence in situ hybridization
GAPDH	Glyceraldehyde-3-phosphate dehydrogenase
HA	Hemagglutinin
HARP	HepA-related protein
HIRA	Histone regulator A
HLTF	Helicase-like transcription factor
HP1	Heterochromatin protein 1
IF	Immunofluorescence

MET-2	Methyltransferase 2
MiDAS	Mitotic DNA synthesis
MMS21	Methyl methanesulfate sensitivity 21
MRN	MRE11-RAD50-NBS1 complex
NaPy	Sodium pyruvate
NF- $\kappa$ B	Nuclear factor $\kappa$ B
NHEJ	Non-homologous end joining
PanNET	Pancreatic neuroendocrine tumor
PARP1	Poly(ADP-ribose) polymerase 1
PBS	Phosphate-buffered saline
PCNA	Proliferating cell nuclear antigen
PIC	Protease inhibitor cocktail
PML	Promyelocytic leukemia
POLD3	DNA polymerase $\delta$ 3, accessory subunit
POT1	Protection of telomeres 1
p/s	Penicillin/streptomycin
PVDF	Polyvinylidene difluoride
RAP1	Repressor and activator protein 1
R-loop	RNA:DNA hybrid
RFC	Replication factor C
RPA	Replication protein A
RPMI	Roswell Park Memorial Institute medium

SDS-PAGE	Sodium dodecyl sulfate–polyacrylamide gel electrophoresis
SETDB1	SET domain bifurcated histone lysine methyltransferase 1
SFB	S-protein-FLAG-biotin
SLX4IP	SLX4-interacting protein
SMARCAL1	SWI/SNF-related, matrix-associated, actin-dependent regulator of chromatin, subfamily A-like 1
SMC5	Structural maintenance of chromosomes 5
SMC6	Structural maintenance of chromosomes 6
SMX	SLX1/SLX4-MUS81/EME1-XPF1/ERCC1 complex
SSC	Saline sodium citrate
SUMO	Small ubiquitin-like modifier
SUV39H	Suppression of variegation 3-9 homologs 1/2
SWI/SNF	Switch/sucrose non-fermenting
TBS	Tris-buffered saline
TERC	Telomerase RNA component
TERRA	Telomere repeat-containing RNA
TERT	Telomerase reverse transcriptase
TIF	Telomere dysfunction-induced foci
TIN2	TRF1-interacting nuclear protein 2
T-loop	Telomere loop
TOP3A	Topoisomerase III $\alpha$
TOPBP1	Topoisomerase II binding protein 1

TPP1	Telomere protection protein 1
TRF1	Telomeric repeat binding factor 1
TRF2	Telomeric repeat binding factor 2
T-SCE	Telomere sister chromatid exchange
XRCC4	X-ray repair cross complementing 4
ZRANB3	Zinc finger ran-binding domain-containing protein 3

## CHAPTER ONE: INTRODUCTION

### Telomere Structure and Function

The linear ends of human chromosomes consist of 10-15 kilobases of repetitive, double-stranded DNA containing repeats of the sequence TTAGGG and its complement<sup>[1]</sup>. This long stretch of double-stranded DNA ends in about 50-300 base pairs of 3' single-stranded overhang<sup>[2]</sup>. This overhang forms a lariat structure by looping back and invading the proximal telomere, creating a telomere loop (T-loop) at the very end of the chromosome<sup>[3]</sup>. The shelterin complex, which has six subunits, structurally facilitates this loop formation and effectively hides the end of the chromosome from being recognized as a DNA break<sup>[4]</sup> (Figure 1). Otherwise, attempts to “repair” the end of the telomere would lead to non-homologous end joining (NHEJ) with other free ends, leading to chromosome fusions and inevitably cell death<sup>[5]</sup>.

The entire shelterin complex is indispensable for preventing activation of any DNA damage response (DDR) triggered by the linear end of the chromosome, and each subunit plays a specific role<sup>[6]</sup>. Telomeric repeat-binding factors 1 and 2 (TRF1 and TRF2) bind double-stranded DNA and are highly specific for the canonical repeats of the telomere sequence<sup>[7,8]</sup>. Protection of telomeres 1 (POT1) binds the single-stranded DNA present in the 3' overhang and displacement loop, also with sequence specificity<sup>[9]</sup>. The complex is stabilized via a bridge formed between TRF1-interacting nuclear protein 2 (TIN2) and POT1 and TIN2 interacting protein (TPP1)<sup>[10]</sup>. Repressor and activator protein 1 (RAP1) binds TRF2 and is thought to help repress telomeric sister chromatid

exchange (T-SCE) and may activate nuclear factor  $\kappa$ B (NF- $\kappa$ B) signaling when displaced from critically shortened telomeres, possibly contributing to senescence signaling<sup>[11]</sup>.

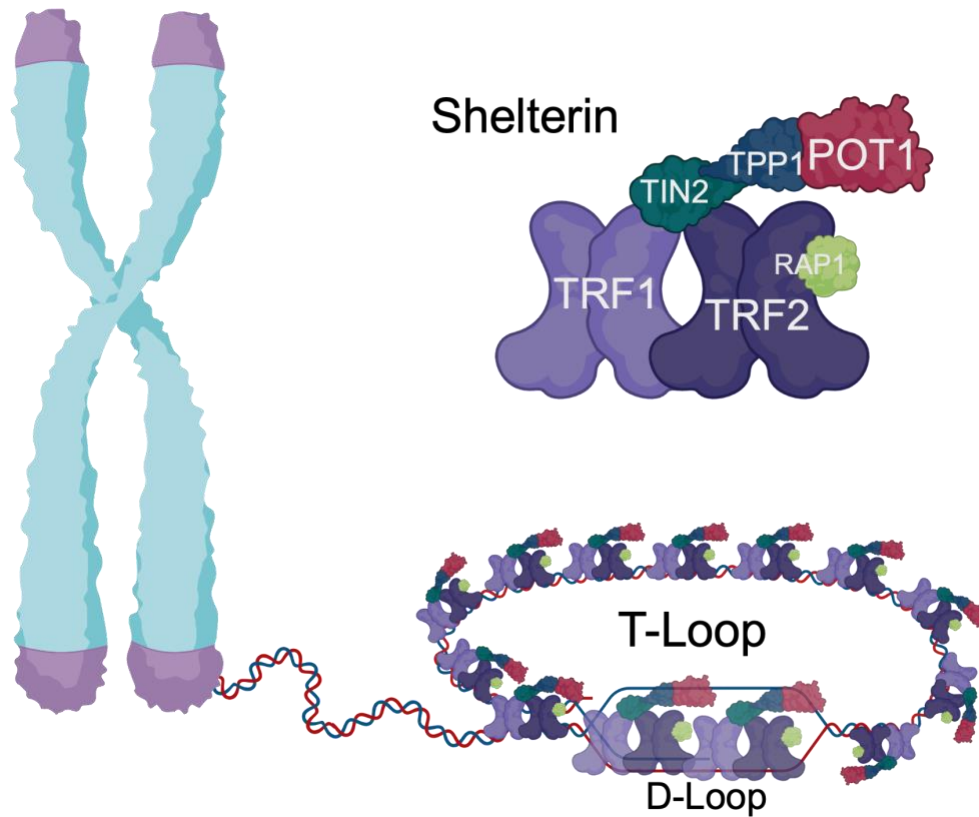


**Figure 1: Telomeres are protected by shelterin-mediated T-loop formation.**

The linear ends of DNA at chromosome termini are sequestered in a T-loop, formed via the six-subunit shelterin complex. Invasion of the proximal telomere by the free 3' overhang creates a D-loop, effectively hiding the end of the telomere. Figure created with BioRender.

## Telomere Maintenance

In 1961, Hayflick and Moorhead proposed that human cells could divide a finite number of times before ceasing to grow and entering a state of replicative senescence, triggered by an intrinsic counting mechanism<sup>[12]</sup>. Later, this counting mechanism was identified as the telomere—thousands of bases of repetitive DNA sequence (TTAGGG) at the end of each chromosome, which are eroded with each round of cell division until reaching a critically short length and sending the cell into a senescent state<sup>[13]</sup>. Telomeric erosion occurs due to both chromosome end processing and the end-replication problem, wherein the replisome cannot fully duplicate the lagging strand due to lack of priming<sup>[14,15]</sup>.

A key function of shelterin and the entire telomeric structure is to repress the DDR via its major damage sensors, ataxia telangiectasia mutated kinase (ATM) and ATM and Rad3-related kinase (ATR). This not only prevents aberrant repair of free chromosome ends, but also prevents activation of the pathways that lead to cellular senescence. An ATM-mediated DDR is typically triggered when its sensor, the MRE11-RAD50-NBS1 (MRN) complex, associates with the free end of a double-stranded break<sup>[16]</sup>. TRF2 specifically represses ATM activation by facilitating T-loop formation, sequestering the free end within a displacement loop (D-loop) and preventing MRN loading<sup>[17]</sup>. Similarly, formation of the T-loop and sequestration of the chromosome end prevent NHEJ by either the classical or alternative pathways, by preventing loading of the Ku70/Ku80 clamp and exclusion of PARP1, respectively<sup>[6,18]</sup>. Briefly, NHEJ can proceed via either classical (c-NHEJ) or alternative (alt-NHEJ) pathways. In most cases, c-NHEJ

is triggered by p53 binding protein 1 (53BP1) and mediated by loading of the Ku70/80 clamp onto free DNA ends. After minimal resection, generally coordinated by DNA-dependent protein kinase catalytic subunit (DNA-PKcs) and the endonuclease Artemis, ends are extended by DNA polymerases  $\mu$  and  $\lambda$  and ligated by the DNA ligase IV-X-ray repair cross complementing 4 (XRCC4) complex. When parts of this machinery are defective, the alternative pathway is triggered after more extensive resection of the break by the MRE11-RAD50-NBS1 (MRN) complex and C-terminal binding protein interacting protein (CtIP), followed by recruitment of poly(ADP-ribose) polymerase 1 (PARP1), which triggers end extension from regions of microhomology by DNA polymerase  $\theta$  and ligation by DNA ligase I or III<sup>[19]</sup>.

POT1, on the other hand, is required to repress signaling by the other DDR kinase, ATR. ATR activation can occur when replication protein A (RPA) binds to single-stranded DNA adjacent to a 5' double-single strand transition area where RAD17 has loaded the RAD9-RAD1-HUS1 (9-1-1) clamp. The ATR recruiter ATRIP binds RPA, bringing ATR in proximity to its activator topoisomerase II binding protein 1 (TOPBP1), which interacts with the 9-1-1 complex<sup>[20]</sup>. ATR can also be activated in the absence of a double-strand/single-strand transition by its other activator, Ewing's tumor-associated antigen 1 (ETAA1), which is brought into proximity with ATRIP and ATR by its interaction with RPA<sup>[21]</sup>. Either of these scenarios can occur in the 3' overhang or D-loop of telomeres, even when in the T-loop conformation, so the shelterin complex is crucial to prevent ATR signaling. POT1 likely outcompetes RPA for binding to ssDNA

following replication within the telomere, thus preventing constitutive activation of ATR<sup>[22]</sup>.

ATR and ATM have a diverse and overlapping set of downstream phosphorylation targets, including CHK1 and CHK2 checkpoint kinases, respectively. The activation of either damage-sensing pathway ultimately leads to stabilization of p53 and halting of the cell cycle<sup>[23]</sup>. This allows time for repair of DNA damage, or if irreparable, permanent cellular senescence or apoptosis. The progressive loss of telomeric DNA with each round of cell division prevents formation of cancer because shortened telomeres become deprotected by shelterin, leading to chronic DDR signaling from chromosome ends and a permanent state of senescence<sup>[24,25]</sup>.

For cancer to develop, cells must avert this telomere dysfunction-triggered senescence. Cancer cells definitionally exhibit growth that is uncoupled from extracellular signals, typically occurring through inactivation of the p53 or pRb pathways<sup>[26]</sup>. When a cell is pushed past the point of senescence by disruption of normal cell cycle checkpoints, it continues to divide until telomeres are truly critically short. This is the point known as telomere crisis, and at this time most cells will begin to accumulate significant genetic alterations as the result of breakage-fusion-bridge cycles from dicentric chromosomes<sup>[27]</sup>. Any cells that survive this stage (approximately 1 in 10 million<sup>[28]</sup>) will have activated a telomere maintenance mechanism, of which there are two main classifications: telomerase reactivation, or alternative lengthening of telomeres (ALT).

### *Telomerase*

Approximately 85-90% of tumors maintain telomere length via reactivation of the enzyme telomerase<sup>[29]</sup>. A reverse transcriptase, this enzyme extends telomeres by simply adding nucleotides to the chromosome ends using its RNA template<sup>[30]</sup>. Telomerase is typically inactivated in differentiated cells, and only found active in the germline and progenitor cells that must maintain a basal amount of cell division for tissue homeostasis<sup>[31]</sup>. The holoenzyme consists of two parts—telomerase reverse transcriptase (TERT) and telomerase RNA component (TERC). TERC is expressed ubiquitously<sup>[32]</sup>, and regulation occurs predominantly at the level of TERT<sup>[33,34]</sup>. Immortalization-driving mutations therefore generally involve re-expression of TERT, and often occur in its promoter<sup>[35]</sup>.

### *Alternative Lengthening of Telomeres*

ALT is defined as telomere extension that occurs in the absence of detectable telomerase activity<sup>[36]</sup>. Estimates for the exact percentage of tumors that rely on this mechanism vary considerably, with 10-15% most often quoted. It is likely, however, that the total percentage of true ALT-positive tumors is only around 4%. This number varies widely by cancer subtype, with the highest rates in cancers of mesenchymal and neuroepithelial origin<sup>[37]</sup>.

The exact molecular mechanisms underlying ALT are poorly understood, but generally resemble break-induced replication (BIR)<sup>[38]</sup>. ALT telomeres experience unusually high rates of replication stress, resulting in stalled replication forks that

collapse into single-ended double-strand breaks. Following resection, the recombinases RAD51 and RAD52 initiate a homology search for a suitable template and facilitate D-loop formation when one is located<sup>[39]</sup>. Branch migration occurs following loading of the proliferating cell nuclear antigen (PCNA) clamp by replication factor C (RFC), allowing for extended DNA synthesis by polymerase  $\delta$ , mediated particularly by its POLD3 accessory subunit<sup>[40]</sup> (Figure 2).

There is strong evidence for branching ALT pathways<sup>[41]</sup>. For example, most ALT-related BIR falls under the category of RAD51-dependent break-induced telomere synthesis (BiTS), occurring throughout the cell cycle. However, other BIR-driven telomere synthesis occurs in a RAD51-independent manner during mitosis; this mitotic DNA synthesis (MiDAS) occurs throughout the genome in response to unresolved replication intermediates, but is particularly prevalent at ALT telomeres and can involve long-tract DNA synthesis<sup>[42,43]</sup>. A recent study has disputed the entire concept of MiDAS, however, demonstrating that it may be an off-target effect of the cyclin-dependent kinase 1 (CDK1) inhibitor RO3306, which seems to nonspecifically inhibit all DNA synthesis. Thus, when this inhibitor is removed from cells to release from G2 arrest, DNA synthesis that had previously been paused can resume, so it appears to be mitotic in origin but is actually just lagging from S-phase<sup>[44]</sup>. Regardless, the diversity of ALT cancers indicates that, although all paths converge on BIR-related telomere synthesis mediated by RAD51 and/or RAD52, the genetic and epigenetic paths to initiation of this telomere elongation mechanism are complicated.

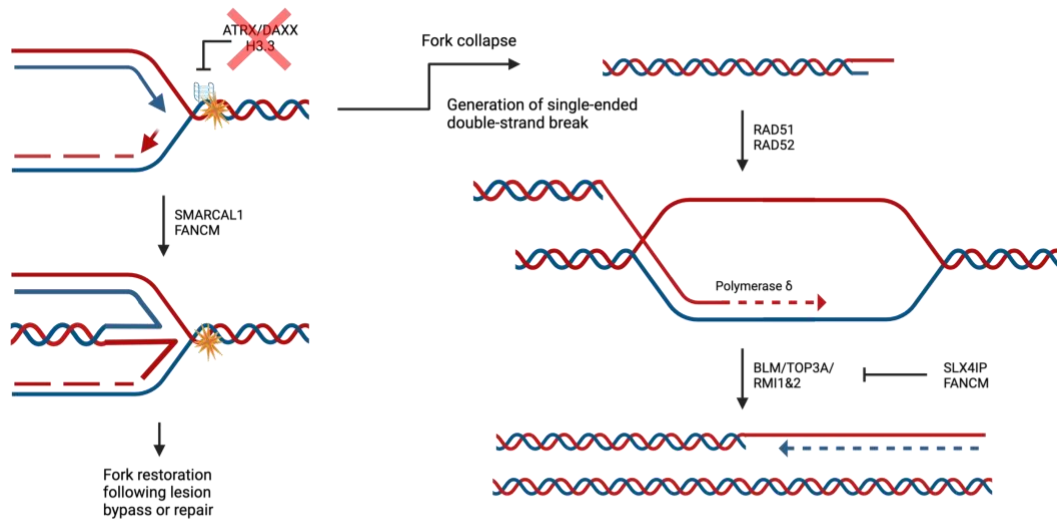


**Figure 2: Schematic of the ALT mechanism.**

At the telomere, a replication fork stalls upon encountering replication stress (for example, G-quadruplex formation that would normally be managed by ATRX/DAXX). Fork reversal by enzymes such as SMARCAL1 and FANCM stabilizes the fork to allow for repair or bypass of the problematic area. If repair is not possible, the fork will collapse into a single-ended double-strand break. Following a homology search by RAD51 or RAD52 recombinases, the free single-stranded end is extended by polymerase  $\delta$ , using another telomere (sister or otherwise) as a template. This hybrid structure is dissolved by the BTR complex, regulated by a number of proteins including SLX4IP and FANCM, for subsequent complementary strand synthesis. Figure created with BioRender.

*Ever-Shorter Telomeres*

It must also be mentioned that a subset of tumors has no detectable telomere maintenance mechanism, possibly representing up to 22% of all cancers<sup>[45–47]</sup>. Likely this is a high estimate, as both telomerase and ALT activity can be difficult to detect, particularly in human cancer tissues. This phenotype is known as ever-shorter telomeres (EST). In some cases, these tumors begin with longer than average telomeres, indicating a possible lengthening event prior to transformation and allowing malignant growth prior to exhaustion of available population doublings<sup>[48]</sup>.

**Telomeric DNA Damage and Replication Stress***Telomeric Replication Stress*

All telomeres undergo chronic replication stress and can be considered common fragile sites in the genome<sup>[49]</sup>. The highly repetitive sequence leads to polymerase slippage and replication errors<sup>[50]</sup>. Additionally, G-quadruplexes form in the G-rich sequence and can act as physical barriers to the replisome<sup>[51]</sup>. The T-loop itself can act as a barrier as well, requiring highly regulated unwinding and reformation with each round of replication<sup>[52]</sup>.

Additionally, telomeres are origin-poor, with the majority of replication originating in the subtelomeric region. Compared with stalled forks in other parts of the genome, forks that stall in the telomere are therefore less likely to be rescued by a

converging fork or dormant origin firing<sup>[53]</sup>. Irreparably stalled forks lead to double-strand DNA breaks that, if not quickly repaired, are detrimental to cell fitness.

### *ALT Replication Stress*

ALT telomeres experience even higher rates of replication stress, resulting in the chronic DNA damage that creates an ALT-permissive state at the telomere<sup>[54,55]</sup>. This predominantly comes from progressive loss of the shelterin complex at ALT telomeres. As ALT telomeres sometimes undergo recombination events with the proximal telomere, into the subtelomeric region, they tend to accumulate degenerate versions of the telomere repeats. These do not effectively bind TRF1 and TRF2, leading to telomeric deprotection<sup>[56]</sup>. TRF1 supports replication efficiency through telomeric DNA and TRF2 has been shown to facilitate the recruitment of the origin recognition complex during replication initiation<sup>[57,58]</sup>. These functions may be limited upon the incorporation of variant repeats and therefore contribute to the replication stress at ALT telomeres.

The identification of the long non-coding telomere repeat-containing RNA (TERRA), transcribed from telomere ends, has added another layer of complexity to replication dynamics in the setting of ALT. The typical, cell cycle-regulated control of TERRA is disrupted in ALT cells, leading to accumulation of RNA:DNA hybrids, or R-loops, that can lead to collision between the transcription bubble and the replisome<sup>[59]</sup>. ALT cells have elevated levels of TERRA at baseline, and inhibiting TERRA transcription decreases ALT phenotypes, indicating that formation of these R-loops may contribute directly to ALT-mediated DNA synthesis<sup>[60,61]</sup>.

An additional source of endogenous replication stress at ALT telomeres is disruption of normal telomeric heterochromatin. The most well-studied ALT-associated mutations occur in the chromatin remodeler ATRX ( $\alpha$ -thalassemia/mental retardation syndrome X-linked) and its histone chaperone partner DAXX (death domain associated protein), which form a complex to deposit histone variant H3.3 in repetitive genomic sequences<sup>[62]</sup>. Loss of H3.3 due to ATRX depletion results in accumulation of G-quadruplex secondary structures and defects in replication fork protection and restart<sup>[63,64]</sup>. Depletion of ATRX renders cells more sensitive to G-quadruplex stabilizing drugs and other sources of DNA damage, including ionizing radiation, alkylating agents, and crosslinking agents<sup>[65-67]</sup>.

Many factors are required to resolve this increased replication stress at ALT telomeres and allow ALT-related telomere elongation events to occur. For example, the ATPase FANCM (Fanconi anemia complementation group M) regulates branch migration activity of the BLM-TOP3A-RMI1/2 (BTR) complex during ALT DNA synthesis<sup>[68]</sup>. Following loss of FANCM, cells display increased telomeric DNA synthesis and an overall increase in ALT activity. This hyper-recombinogenic phenotype ultimately leads to cell death<sup>[68-70]</sup>. Notably, disruption of the interaction between Bloom's helicase (BLM) and FANCM is sufficient to recapitulate this uncontrolled DNA synthesis and replication stress, indicating that FANCM prevents excessive BLM-mediated ALT DNA synthesis<sup>[69]</sup>. The Fanconi anemia complementation groups A and D2 proteins (FANCA and FANCD2), also involved in stalled fork restart, may be required for ALT DNA synthesis as well<sup>[71]</sup>. Other proteins required for recombination-

dependent replication fork restart include flap endonuclease 1 (FEN1)<sup>[72]</sup>, the crossover junction endonuclease MUS81<sup>[73]</sup>, and the annealing helicase SMARCAL1 (SWI/SNF-related, matrix-associated, actin-dependent regulator of chromatin, subfamily A-like 1)<sup>[74]</sup>.

### *Hallmarks of ALT*

There is no single diagnostic test to determine if a tumor or cultured cell line is ALT-positive. In addition to an absence of telomerase activity, however, several phenotypes unite ALT cancers<sup>[54]</sup>.

A unique feature of ALT telomeres is that they cluster in ALT-associated promyelocytic leukemia (PML) bodies (APB)<sup>[75]</sup>. In general, PML bodies are found in most cell lines and act as platforms for SUMOylated (small ubiquitin-like modifier) proteins involved in diverse processes from transcription to apoptosis<sup>[76]</sup>. In telomerase-positive tumors, the telomeres are excluded from these structures. ALT telomeric inclusion in PML bodies, accompanied by the presence of histone  $\gamma$ H2AX (variant H2AX phosphorylated at serine 139, an early event in the DDR<sup>[77]</sup>) and the 9-1-1 complex, is representative of the fact that these telomeres are being recognized as double-strand breaks, and that APBs are sites of attempted repair<sup>[78]</sup>. The structural maintenance of chromosomes 5/6 (SMC5/6) complex and its SUMO E3 ligase, methyl methanesulfonate sensitivity 21 (MMS21), are required for ALT telomere synthesis and seem to drive telomere recruitment into APBs via SUMOylation of shelterin<sup>[79]</sup>. Strikingly, targeting of overexpressed BLM into artificial PML body constructs is sufficient to induce DNA synthesis via telomeric MiDAS<sup>[43]</sup>, and tethering PML to TRF1 induces telomere

clustering and telomeric DNA synthesis<sup>[80]</sup>. Although this may be confounded by off-target effects from RO3306 cell synchronization<sup>[44]</sup>, these findings emphasize that APB should be thought of not only as a symptom, but a driving factor, of ALT.

ALT tumors also produce extra-chromosomal, partially single-stranded, C-rich, circular DNA products known as C-circles. Although not known exactly what these represent, they are almost certainly byproducts of ALT-recombination and are seen exclusively in ALT tumors<sup>[81]</sup>. They are self-priming, can be amplified by rolling-circle amplification and quantified by southern blot<sup>[82]</sup>. C-circle levels are thought to correlate with the amount of ALT activity occurring in each cell line or tumor and have been detected in patient blood samples<sup>[81,83]</sup>. ALT activity also produces other varieties of extrachromosomal DNA containing the telomere sequence, in the form of double-stranded T-circles, partially single-stranded G-circles, linear fragments of double-stranded DNA, and various branched structures<sup>[84-87]</sup>.

Overall, ALT-elongated telomeres are more variable in length than those extended by telomerase and change more dynamically<sup>[36,88]</sup>. ALT telomeres also undergo frequent recombination events with other telomeres, therefore demonstrating higher rates of telomere sister chromatid exchange (T-SCE) than telomerase-positive cancers<sup>[89,90]</sup>. Overall, telomeres that undergo extension via ALT exhibit phenotypes consistent with high rates of DNA damage and ongoing repair processes.

## Genetics of ALT

No single mutation drives a cell to activate ALT as a telomere maintenance mechanism, but there are several characterized mutations that correlate closely with development of ALT and contribute to its associated phenotypes (Table 1). Likely, these mutations induce ALT when they occur in a specific genetic or epigenetic background.

### *ATRX/DAXX*

The most well-characterized ALT-associated mutations occur in the ATRX/DAXX histone H3.3 deposition pathway<sup>[62,91–93]</sup>. Histone variant H3.3 is deposited by ATRX and its specific histone chaperone, DAXX, in a replication-independent manner at the telomere<sup>[94]</sup>. When deposited by its other chaperone, histone regulator A (HIRA), H3.3 is associated with active genes, promoters, and regulatory elements, and is thought to be involved in transcription regulation<sup>[95]</sup>. However, at the telomeres, where transcription is generally repressed, H3.3 is deposited by ATRX/DAXX in a HIRA-independent manner<sup>[96]</sup>. The exact mechanism by which ATRX/DAXX mutations drive the ALT phenotype is unknown. However, the fact that HIRA can perform compensatory H3.3 deposition without resolving telomeric replication stress suggests that ATRX represses ALT by other means<sup>[97]</sup>. Loss of ATRX disrupts the cell's ability to repress G-quadruplex formation<sup>[65,64]</sup> and de-regulates transcription of the long non-coding RNA TERRA<sup>[58]</sup>, leading to telomeric R-loops and increasing at least two potential replisome barriers that may cause fork stalling and initiate ALT elongation events.

*SLX4IP & TOP3A*

Four-way Holliday junction DNA structures resulting from reversed replication forks can either be resolved by the SLX1/SLX4-MUS81/EME1-XPF1/ERCC1 (SMX) structure-specific endonuclease complex, yielding crossover and non-crossover events<sup>[98]</sup>, or dissolved by the BTR complex in a way that limits crossover<sup>[99]</sup>. The balance between these two mechanisms of resolution at telomeres is dependent on SLX4 interacting protein (SLX4IP), which interacts with both complexes. In its absence, BLM activity occurs in an unchecked manner, promoting ALT activity via dissolution of BIR-induced DNA structures. Loss of SLX4IP is seen in a subset of ALT-positive osteosarcomas without other known ALT-associated mutations<sup>[100]</sup>.

In addition to loss of SLX4IP, overexpression of the BTR component topoisomerase III $\alpha$  (TOP3A) has also been implicated in driving cells toward initiation of ALT. Amplification of the chromosome region containing TOP3A appears in a large subset of ALT-positive high-grade pediatric osteosarcomas, demonstrating another case where overactive BTR activity can lead to ALT DNA synthesis<sup>[101]</sup>.

*SMARCAL1*

A final ALT-associated mutation, lost in some osteosarcoma cell lines and glioblastoma tumors, occurs in the annealing helicase SMARCAL1<sup>[102-104]</sup>. The primary function of this enzyme is to reverse and stabilize stalled replication forks throughout the genome<sup>[105-107]</sup>. Initially known as HepA-related protein (HARP), SMARCAL1 contains two DNA-binding HARP domains, which provide specificity for double-stranded/single-stranded DNA junctions<sup>[108]</sup>. It is a member of the SNF2 chromatin remodeling family of

proteins, containing a switch/sucrose non-fermenting (SWI/SNF) helicase domain. However, unlike most other members of this family, the ATPase-driven function of SMARCAL1 anneals, rather than unwinds, DNA<sup>[109]</sup>. This highly specific function is dictated by the HARP domains, artificial chimeric fusion of which can induce DNA annealing activity in other SNF2 ATPases<sup>[108]</sup>. Although two other SNF2 annealing helicases, ZRANB3 (zinc finger ran-binding domain-containing protein 3) and HLTF (helicase-like transcription factor), are closely related and share similar fork reversal functions, only SMARCAL1 appears to act at telomeres<sup>[110]</sup>. The ATPase domain is necessary for both fork remodeling and repression of ALT phenotypes<sup>[102,106]</sup>.

SMARCAL1 specifically anneals single-stranded DNA coated in RPA<sup>[109,111]</sup>. At the N-terminus, SMARCAL1 contains an RPA-binding domain, which is necessary and sufficient for recruitment to stalled forks containing stretches of RPA-coated single-stranded DNA<sup>[106,111]</sup>. Oddly, the entire N-terminus of the protein appears to be dispensable for both recruitment to telomeres and repression of ALT phenotypes<sup>[102,110]</sup>, indicating a possible separate mechanism of recruitment and function at the telomeres.

#### *SMARCAL1 and ALT*

Prior to being identified as a protein lost in ALT tumors, SMARCAL1 was shown to actually aid in propagation of ALT, being necessary to resolve the unusually high rates of replication stress that occur at ALT telomeres. In its absence, an accumulation of unresolvable stalled forks leads to cleavage by the SMX complex, and eventual end-to-end chromosome fusions<sup>[74]</sup>.

Gene	Function	ALT-associated mutation	Tumor type
ATRX	H3.3 deposition, G-quadruplex resolution	Loss of function	PanNETs, low-grade glioma, glioblastoma multiforme, neuroblastoma, osteosarcoma, adrenocortical tumors, leiomyosarcoma, angiosarcoma, liposarcoma <sup>[112]</sup>
DAXX	H3.3-specific histone chaperone	Loss of function	PanNETs, glioblastoma multiforme, adrenocortical carcinoma, osteosarcoma <sup>[112]</sup>
SLX4IP	Facilitates SMX-mediated fork resolution, antagonizes BT-mediated dissolution	Loss of function	osteosarcoma <sup>[100]</sup>
TOP3A	BTR dissolvasome topoisomerase	Amplification	osteosarcoma <sup>[101]</sup>
SMARCAL1	Stalled replication fork reversal	Loss of function	glioblastoma multiforme, osteosarcoma <sup>[102,104]</sup>

**Table 1. Major ALT-associated mutations**

This may seem paradoxical, considering that a subset of ALT tumors and cell lines exhibit loss of SMARCAL1. However, even in cells where it is required to resolve replication stress, its loss leads to an increase in ALT phenotypes like APB formation, RAD51-driven telomere clustering, and C-circle production<sup>[74]</sup>. It is therefore understandable how loss of this protein during the process of immortalization could push cells toward development of the ALT phenotype.

### **Concluding Remarks**

Compared with telomerase re-activation, the molecular mechanisms underlying induction and perpetuation of the ALT pathway are poorly understood. Although utilized by a relatively small percentage of tumors overall, ALT is highly prevalent in some cancer subtypes, including osteosarcomas, pancreatic neuroendocrine tumors (PanNET), and tumors of the central nervous system. Furthermore, the prognosis for ALT-positive tumors varies by cancer type. In glioblastoma, ALT-positivity correlates with longer survival, while in sarcomas and non-functional (non-hormone hypersecreting) PanNETs, ALT-positivity correlates with worse overall prognosis<sup>[113-117]</sup>. This difference in patient outcomes indicates an urgent need for development of specific therapeutic options. The vulnerability of ALT cancers to any disruption in the DDR is a clear Achilles heel of these tumors<sup>[55,59]</sup>, potentially opening the door for highly specific treatments if the underlying mechanisms can be teased apart. In particular, the stress response helicase SMARCAL1 has a complicated and poorly understood role at ALT telomeres, which we sought to further elucidate with this body of work.

### *Hypothesis and Aims*

The primary goal of this work was to gain mechanistic insight into the role of SMARCAL1 at ALT telomeres. If ALT is truly a consequence of H3.3 loss at telomeres, which is the prevailing view, we would expect SMARCAL1 loss to have similar effects to ATRX/DAXX loss in this regard. Given that SMARCAL1 and ATRX are both in the SNF2 helicase family, we hypothesized that they may have overlapping functions in chromatin maintenance at ALT telomeres. To address this hypothesis, we had two main

aims. First, we wanted to know if SMARCAL1 loss led to chromatin alteration in terms of histone deposition or modification. Second, after discovering a novel interaction between SMARCAL1 and heterochromatin protein 1 (HP1), we asked if this interaction had functional consequences at the telomere. Taken together, the goal of these aims was to provide further insight into the molecular mechanisms that create an ALT-permissive state at the telomere, and specifically to obtain a better understanding of the increasingly complicated telomeric role of SMARCAL1.

## **CHAPTER TWO: SMARCAL1 CONTRIBUTES TO TELOMERIC HETEROCHROMATIN MAINTENANCE**

### **Abstract**

ALT telomeres rely on chronic replication stress to initiate DDR-mediated telomere elongation events. Although it is known that the annealing helicase SMARCAL1 is important for both maintenance of the ALT pathway and repression of excessive ALT activity, the molecular mechanisms of this are not presently clear. In this work, we sought to further define the function of SMARCAL1 at telomeres. We found that ALT cells are particularly sensitive to combined depletion of SMARCAL1 and the canonical ALT repressor ATRX. In exploring possible causes of this susceptibility, we found that knockdown of either ATRX or SMARCAL1 leads to similar loss of a heterochromatic mark, trimethylated lysine 9 of histone 3 (H3K9me3), in non-ALT cells. This indicates a previously undescribed role for SMARCAL1 in heterochromatin maintenance at the telomere.

### **Introduction**

Cancer cells require a mechanism of telomere elongation to support prolonged cell division and avoid replicative senescence<sup>[26]</sup>. To achieve this, a minority of tumors rely on the ALT pathway, which uses homologous recombination between telomeres to mediate extension events<sup>[36]</sup>. It has been described as resembling BIR, which is activated following a single-ended double-strand DNA break resulting from replication fork collapse<sup>[38]</sup>.

All telomeres undergo chronic replication stress due to their repetitive sequence and propensity to form secondary structures, like G-quadruplexes<sup>[57]</sup>. ALT telomeres, which accumulate interspersed degenerate repeats, experience higher rates of replication stress due to loss of the protective shelterin complex<sup>[6,56]</sup>. They therefore rely heavily on factors that protect, stabilize, and resolve stalled replication forks, including the annealing helicase SMARCAL1.

SMARCAL1 was previously shown to be critical for resolution of replication stress at ALT telomeres. In its absence, there is an increase in DNA damage signaling, cleavage of persistently stalled forks by the SMX complex, and chromosome fusions resulting from fork collapse<sup>[74]</sup>. Conversely, a subset of ALT tumors and cell lines have lost SMARCAL1 expression entirely<sup>[102,104]</sup>.

Canonical ALT-associated mutations occur in the ATRX/DAXX histone H3.3 deposition complex<sup>[91]</sup>. ATRX and SMARCAL1 are both SNF2 helicases, but do not have any known overlap in specific function. Therefore, we wondered if SMARCAL1 loss and ATRX loss resulted in similar phenotypes regarding histone deposition or other chromatin architecture. Generally, SMARCAL1 is recruited to sites of DNA damage via its RPA-binding domain, which interacts with stretches of single-stranded DNA coated with RPA that form at stalled replication forks<sup>[111]</sup>. This domain is unnecessary for recruitment to telomeres, however, and seems dispensable for repression of ALT phenotypes<sup>[102,110]</sup>. Since this implies the possibility of a divergent telomeric function of SMARCAL1, we asked if it possibly played a direct role in chromatin maintenance at telomeres.

## Materials and Methods

### *Cell Lines and Culture Conditions*

All cell lines were grown in a 37°C humidified incubator with 5% CO<sub>2</sub>. Cells were grown in Dulbecco's modified Eagle medium (DMEM) with or without nutrient mixture F-12, Roswell Park Memorial Institute medium 1640 (RPMI), or Eagle's minimum essential medium (EMEM). Media were reconstituted with added fetal bovine serum (FBS), penicillin/streptomycin (p/s), and sodium pyruvate (NaPy) (Table 2).

<b>Cell Line</b>	<b>Origin</b>	<b>TMM</b>	<b>Culture medium</b>	<b>ALT-related mutation</b>
CAL72	osteosarcoma	ALT	DMEM/F-12, 10% FBS, 1% p/s	ATRX
CAL78	chondrosarcoma	ALT	RPMI, 10% FBS, 1% p/s, 1% NaPy	SMARCAL1
G292	osteosarcoma	ALT	RPMI, 5% FBS, 1% p/s, 1% NaPy	DAXX <sup>[103]</sup>
GM847	skin fibroblast (SV40-transformed)	ALT	EMEM, 10% FBS, 1% p/s	ATRX
HCT116	colorectal carcinoma	telomerase	DMEM, 10% FBS, 1% p/s	N/A
HEK293	embryonic kidney	telomerase	DMEM, 10% FBS, 1% p/s	N/A
HeLa 1.2.11 (HeLaLT)	cervical carcinoma	telomerase	DMEM, 10% FBS, 1% p/s	N/A
HOS	osteosarcoma	telomerase	EMEM, 10% FBS, 1% p/s	N/A
HUO3N1	osteosarcoma	EST	RPMI, 10% FBS, 1% p/s, 1% NaPy	N/A

HUO9	osteosarcoma	ALT	RPMI, 5% FBS, 1% p/s, 1% NaPy	ATRX
MG63	osteosarcoma	telomerase	DMEM/F-12, 5% FBS, 1% p/s	N/A
NOS1	osteosarcoma	ALT	RPMI, 5% FBS, 1% p/s, 1% NaPy	ATRX
NY	osteosarcoma	ALT	DMEM/F-12, 5% FBS, 1% p/s	SMARCAL1
SaOS2	osteosarcoma	ALT	RPMI, 10% FBS, 1% p/s	ATRX
SJSA1	osteosarcoma	telomerase	RPMI, 5% FBS, 1% p/s, 1% NaPy	N/A
SKLU-1	lung adenocarcinoma	ALT	DMEM/F-12, 5% FBS, 1% p/s	unknown
SW13	IMR90 fetal lung fibroblast (SV40-transformed)	ALT	DMEM, 10% FBS, 1% p/s	unknown
SW26	IMR90 fetal lung fibroblast (SV40-transformed)	ALT	DMEM, 10% FBS, 1% p/s	ATRX
SW39	IMR90 fetal lung fibroblast (SV40-transformed)	telomerase	DMEM, 10% FBS, 1% p/s	N/A
U2OS	osteosarcoma	ALT	DMEM, 10% FBS, 1% p/s	ATRX
VA13	fetal lung fibroblast (SV40-transformed)	ALT	EMEM, 10% FBS, 1% p/s	ATRX

**Table 2. Cell lines used**

### *siRNA Transfection*

Cells were transfected using Lipofectamine RNAiMax (Thermo Fisher) diluted in Opti-MEM reduced serum medium (Gibco) per manufacturer's instructions, using siRNAs at a final concentration of 20 nM in cellular growth medium (unless otherwise

noted). Approximately 24 hours post-transfection, diluted siRNA was removed and replaced with fresh medium. Pellets were collected 72 hours post-transfection for knockdown confirmation.

siRNAs used:

control: Silencer Select Negative Control No. 1 siRNA (Ambion/Invitrogen  
4390843)

SMARCAL1: Dharmacon custom, targets 3' untranslated region  
(UUU CAC AGA GAA AUG CUU AUG CAG GU)

ATRX: Invitrogen Stealth RNAi targeting NM\_000489.3

DAXX: Dharmacon/Horizon Discovery J-004420-08  
(GGA GUU GGA UCU CUC AGA A)

#### *Plasmid Overexpression*

Cells were transfected using FuGENE reagent (Promega) diluted in Opti-MEM reduced serum medium (Gibco) per manufacturer's instructions. Generally, 2 µg plasmid DNA was used for transfection of one well of a 6-well plate, and 10 µg plasmid DNA was used for transfection in a 10 cm dish. Diluted transfection complexes were replaced with fresh culture medium approximately 24 hours after addition. Pellets were collected for western blot to analyze expression 48-72 hours post-transfection. Plasmids used: pLPC-NMYC-TRF2 (Addgene #16066).

*Lentiviral Infection/shRNA-Mediated Knockdown*

HEK293FT cells were plated in a 6-well dish ( $5 \times 10^5$  cells per well). After 24 hours, cells were transfected with 2.5  $\mu\text{g}$  psPAX2, 0.5  $\mu\text{g}$  pMD2.G, and 2  $\mu\text{g}$  shRNA-containing plasmid DNA using FuGENE Transfection Reagent (Promega), diluted in Opti-MEM reduced serum medium per manufacturer's instructions. Cells were incubated with transfection complexes for four hours before replacement with fresh medium. After 36-48 hours, virus-containing media was filtered onto cells to be infected through 0.45  $\mu\text{m}$  filter. Polybrene was added to a final concentration of 8  $\mu\text{g}/\text{mL}$ . After 24 hours, the virus was replaced with fresh culture medium. For cell lines stably expressing an inducible shRNA against SMARCAL1, puromycin (0.2-10  $\mu\text{g}/\text{mL}$ ) was added for selection an additional 24 hours later. After selection, 2  $\mu\text{g}/\text{mL}$  doxycycline was added to culture medium to induce knockdown of SMARCAL1. Pellets were collected 72 hours after infection or doxycycline addition, unless otherwise indicated, to assess knockdown efficiency. Plasmids used: control (pLKO.1 empty vector), shATRX (Sigma MISSION TRCN0000013592), shSMARCAL1 (Dharmacon SMARTvector hEF1a-TurboGFP shRNA), shSETDB1 (Sigma MISSION TRCN0000276105).

*Western Blots*

Cells were lysed in NETN buffer (100 mM NaCl, 20 mM Tris-HCl pH 8.0, 0.5 mM EDTA, 0.5% NP-40) with added protease inhibitor cocktail (PIC - Sigma Aldrich). After incubation on ice for 15-30 minutes, lysates were sonicated for 20 seconds at 20% amplitude with probe sonicator, then centrifuged at high speed, 4C, for 10 minutes. Supernatant was boiled at 95C in 1X Bolt LDS Sample Buffer (Invitrogen). Dithiothreitol

(DTT) was added to 100 mM. Protein samples were resolved by sodium dodecyl sulfate–polyacrylamide gel electrophoresis (SDS-PAGE) and transferred to a polyvinylidene difluoride (PVDF) membrane (250 mA for one hour or 30 mA overnight). Membranes were blocked in Tris-buffered saline with 0.1% TWEEN-20 (TBS-T) and 5% nonfat dry milk for at least 30 minutes prior to incubation overnight with primary antibodies, also diluted in TBS-T with 5% milk. Blots were subsequently washed three times with TBS-T, incubated in horseradish peroxidase-conjugated antibody diluted 1:8000 in TBS-T with 5% milk for 1 hour, and washed three times again before development with Clarity Western ECL Substrate (Bio-Rad). Antibodies used: ATRX (diluted 1:500, Cell Signaling 14820S), SMARCAL1 (diluted 1:250, Santa Cruz sc-376377), DAXX (diluted 1:500, Cell Signaling 25C12 or Bethyl A301-353A),  $\alpha$ -tubulin (diluted 1:1000, Cell Signaling 2125S), GAPDH (diluted 1:1000, Santa Cruz sc-47724), c-MYC (diluted 1:1000, Thermo MA1-980), SETDB1 (diluted 1:500, proteintech 11231-1-AP).

#### *Luminescence-Based Viability Assay*

For siRNA knockdown, cells were plated and reverse transfected on day 0, then forward transfected again on day 4. For shRNA knockdown, cells were infected with shATRX-containing virus on day 0 and SMARCAL1 knockdown was induced with doxycycline addition on day 1. When cells reached confluency, 100-1000 cells per well were transferred to 96-well plates. Three wells for each condition were used per biological replicate. Viability assays were carried out on day 7 using CellTiter-Glo reagent (Promega) per manufacturer instructions.

*Immunofluorescence-Fluorescence in situ Hybridization (IF-FISH)*

Cells growing on glass coverslips were washed twice for 5 minutes each with phosphate buffered saline (PBS). Coverslips were then washed with cold cyotobuffer (100 mM NaCl, 300 mM sucrose, 3 mM MgCl<sub>2</sub>, 10 mM PIPES, 0.1% Triton X-100) for about one minute before being fixed in 4% paraformaldehyde in PBS for 10 minutes at room temperature. Cells were then washed briefly in PBS and permeabilized using 0.1% Triton X-100 for 10 minutes at room temperature. Cells were blocked in PBS with 0.5% bovine serum albumin (BSA) and 0.2% fish gelatin (PBG buffer) for either 1 hour at room temperature or for longer term storage at 4C. Coverslips were incubated in primary antibodies diluted in PBG overnight at 4C, washed three times with PBS, incubated with secondary fluorescent-conjugated antibodies diluted in PBG buffer at room temperature for 1 hour, then washed three times again with PBS. Cells were fixed again with 4% paraformaldehyde in PBS for 10 minutes at room temperature, then rinsed with PBS. For FISH, cells were treated with 100 µg/mL RNase A diluted in PBS for 30 minutes at 37C. Cells were then dehydrated in a 70%-85%-100% series of ethanol washes for 2 minutes each, then coverslips were allowed to dry fully at room temperature. Coverslips were then flipped onto glass slides over spotted TelC-Cy3 probe (PNA Bio F1002) diluted 1:500 in denaturing buffer (56% formamide, 0.12% Roche blocking reagent, 8 mM Tris pH 7.5, 4.1 mM Na<sub>2</sub>HPO<sub>4</sub>, 1.25 mM MgCl<sub>2</sub>, 4.5 mM citric acid) and denatured at 85C for 10 minutes. Slides were left overnight at room temperature for hybridization. Coverslips were then washed three times in 2X saline-sodium citrate (SSC) with 50% formamide and three times in 2X SSC at 37C. Cells were counterstained with 4',6-diamidino-2-

phenylindole (DAPI) in 2X SSC for 10 minutes at room temperature, then mounted on slides with VECTASHIELD mounting medium and sealed. Images were taken using a Zeiss LSM 710-Live Duo Scan microscope. Primary antibodies: ATRX (diluted 1:500, Santa Cruz sc-55584). Secondary antibodies (all diluted 1:250): Donkey anti-mouse IgG AlexaFluor 488 (Jackson ImmunoResearch or abcam). Foci were counted by eye using ImageJ software or automatically using CellProfiler software from the Broad Institute.

#### *Chromatin Immunoprecipitation (ChIP)*

Cells were treated for knockdown or overexpression as indicated. In general, 1-2 confluent 10 cm tissue culture dishes were used for each condition in HeLaLT experiments, and 3 confluent 10 cm culture dishes for VA13. Formaldehyde was added directly to culture medium to a final concentration of 1% and incubated at room temperature for 8 minutes to crosslink DNA and proteins. Crosslinking was quenched by adding glycine to a final concentration of 0.125M and allowing to incubate an additional 5 minutes at room temperature. Dishes were washed twice with cold PBS, then collected in PBS by scraping. Cells were pelleted (800 rpm for 5 minutes at 4C), resuspended in cellular lysis buffer (5 mM PIPES, 85 mM KCl, 0.5% NP-40) with PIC (Sigma Aldrich), and incubated on ice for 5 minutes. Nuclei-enriched pellets were obtained by centrifugation (800 rpm for 5 minutes at 4C) and resuspended in nuclear lysis buffer (50 mM Tris-HCl pH 8.0, 10 mM EDTA pH 8.0, 0.2% SDS) with added PIC. Chromatin was sonicated for 45-85 minutes to obtain fragments between 100 and 500 base pairs in length and then sonicated at high speed for 10 minutes at 4C to clear debris. 2-10  $\mu$ g of antibody was incubated with 300  $\mu$ g of chromatin in nuclear lysis buffer with PIC overnight at 4C.

Samples were then diluted by one third with dilution IP buffer (16.7 mM Tris-HCl pH 8.0, 1.2 mM EDTA, 167 mM NaCl, 0.01% SDS, 1.1% Triton X-100) and incubated with 40  $\mu$ L pre-washed protein A (for rabbit antibodies) or G (for mouse antibodies) beads (New England Biolabs or Invitrogen Dynabeads) for 2 hours at 4C. Beads were collected and washed twice with dilution IP buffer, once with TSE buffer (20 mM Tris-HCl pH 8.0, 2 mM EDTA pH 8.0, 500 mM NaCl, 1% Triton X-100, 0.1% SDS), once with LiCl buffer (100 mM Tris-HCl pH 8.0, 500 mM LiCl, 1% sodium deoxycholate, 1% Nonidet P-40), and twice with TE buffer (10 mM Tris-HCl pH 8.0, 1 mM EDTA pH 8.0). Beads and input samples were then resuspended in 150  $\mu$ L elution buffer (50 mM NaHCO<sub>3</sub>, 140 mM NaCl, 1% SDS) with added Proteinase K (10  $\mu$ g/sample) and shaken in thermomixer at 55C for 1 hour. Beads were removed with magnet and remaining chromatin was digested at 65C overnight. Each chromatin sample was treated with 200  $\mu$ g RNase A and shaken at 37C for 30 minutes in thermomixer. DNA was isolated using QIAquick PCR Purification Kit (QIAGEN) and each sample was eluted in 50  $\mu$ L water. After boiling for 5 minutes to denature DNA, SSC was added to a final concentration of 10X. Samples were run through dot blot apparatus (Bio-Rad) onto Amersham Hybond N+ membrane (GE Healthcare) and DNA was crosslinked to membrane for 35 seconds. Membrane was blocked in ULTRAhyb buffer (Invitrogen) for at least 30 minutes and then incubated with oligonucleotide probe diluted in ULTRAhyb buffer overnight at 50C. Blot was developed using DIG Wash and Block Buffer Set with anti-Digoxigenin-AP Fab fragments and CDP-Star chemiluminescent substrate (Roche) per manufacturer instructions. Signal was quantified using BioRad ImageLab 6.1 software. Antibodies

used for IP: H3.3 (2 µg, abcam 176840), H3K9me3 (Millipore 07-442, 2-10 µg per IP), c-Myc (Thermo MA1-980, 2 µg per IP), IgG (Diagenode C15410206, 2 µg per IP), TRF2 (Bethyl A300-796A, 2 µg per IP). Oligonucleotide probes for southern dot blot: telomere (CCCTAA)<sub>4</sub> and Alu (GTGATCCGCCCGCCTCGGCCTCCCAAAGTG) from Invitrogen, labeled using DIG Oligonucleotide 3'-End Labeling Kit (Roche) components 1-4 per manufacturer instructions.

### *Statistical Analysis*

Statistical analysis was carried out in GraphPad Prism, as indicated in figure legends. Two-condition experiments were compared by unpaired t test; those with more than two conditions were compared by one-way ANOVA with appropriate multiple comparisons testing. *P*-values of < 0.05 were considered significant.

## **Results**

### *SMARCAL1 loss does not affect ATRX localization to telomeres or H3.3 deposition*

Our initial goal was to understand how loss of SMARCAL1 led to the same ALT phenotypes as ATRX defects. To do this, we used the 1.2.11 HeLa subclone line (referred to as HeLaLT throughout), which utilize telomerase but have telomeres that are unusually long, similar in length to some ALT cells. Our main goal in using this line was to find a phenotype in a telomerase-positive cell line that might indicate that loss of SMARCAL1 was, if not strictly inducing ALT, at least leading to development of ALT-like phenotypes. First, we wanted to rule out the possibility that SMARCAL1 depletion

disrupted ATRX localization to telomeres. In telomerase-positive HeLaLT cells harboring inducible shRNA against SMARCAL1, five-day knockdown of SMARCAL1 did not change the frequency of ATRX co-localization with telomeres (Figure 3 A-B). Furthermore, our SMARCAL1-deficient cell lines, NY and CAL78, had definite ATRX foci at telomeres (Figure 3 C-D). Therefore, it is unlikely that SMARCAL1 loss is driving ALT by somehow interrupting localization of canonical H3.3 deposition machinery to the telomere.

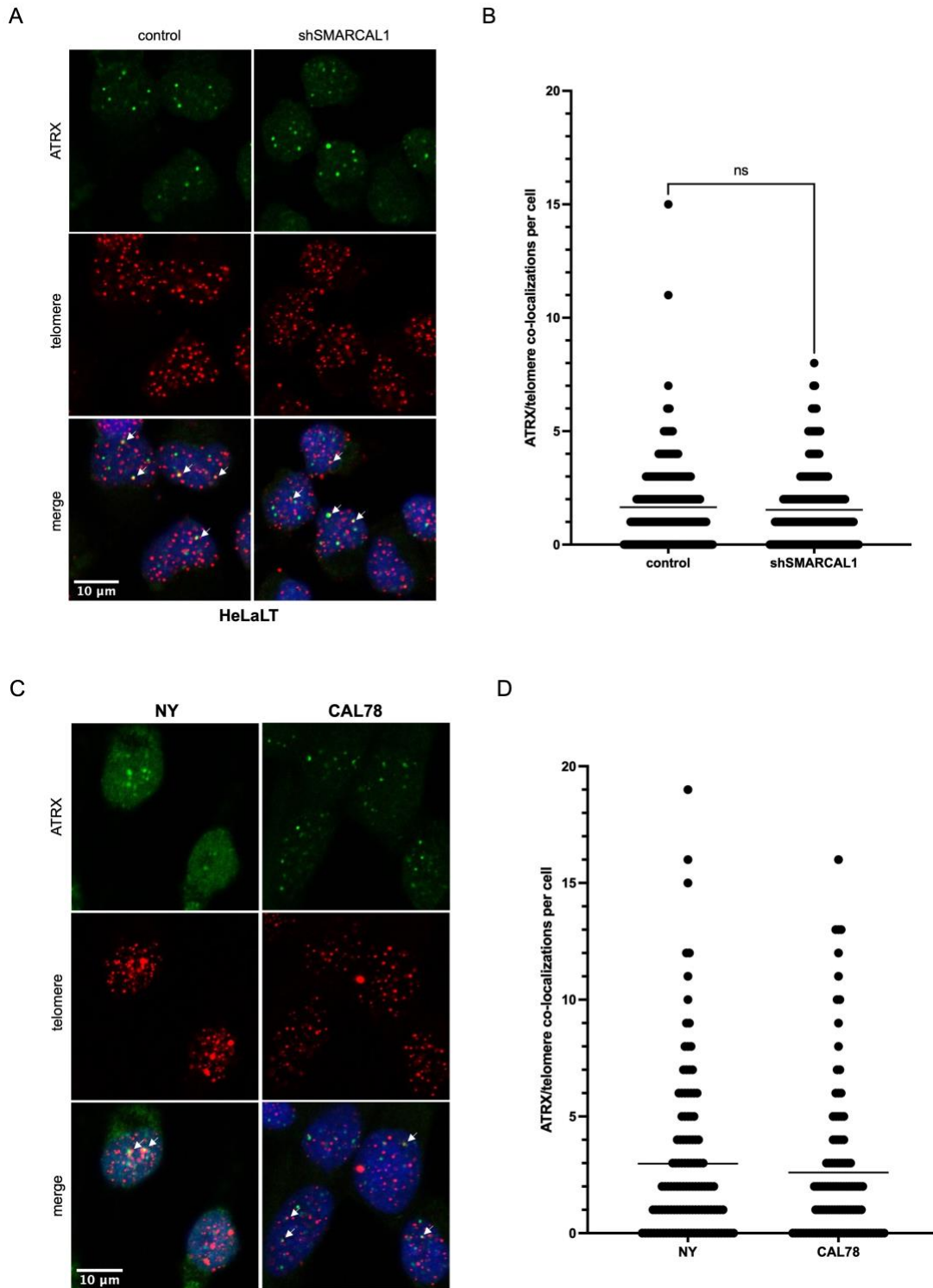


**Figure 3: SMARCAL1 loss does not displace ATRX from telomeres.**

- A. Representative IF-FISH images of HeLaLT cells stained for ATRX (IF) and telomeres (FISH), and counterstained with DAPI. SMARCAL1 knockdown was induced for 5 days by growth in media with 2  $\mu\text{g}/\text{mL}$  doxycycline. White arrows indicate co-localization of ATRX with telomere signal.
- B. Quantification of data from A. Each dot represents number of ATRX-telomere co-localizations from one cell. Line represents mean number of co-localizations per cell. At least 100 cells were counted for each of three biological replicates.  $p = 0.3317$ , unpaired t test.
- C. Representative IF-FISH images of NY and CAL78 cells stained for ATRX (IF) and telomeres (FISH), and counterstained with DAPI. White arrows indicate co-localization of ATRX with telomere signal.
- D. Quantification of data from D. Each dot represents number of ATRX-telomere co-localizations from one cell. Line represents mean number of co-localizations per cell. 100-200 cells were counted for each cell line.

Since the main role of ATRX and DAXX is to deposit H3.3 in repetitive regions of the genome, we asked if loss of SMARCAL1 would similarly lead to loss of H3.3 at telomeres. In HeLaLT cells with doxycycline-inducible shRNA against SMARCAL1, we induced knockdown or treated with an siRNA against DAXX, then performed ChIP for H3.3 after six days. We found that, as expected, DAXX knockdown resulted in a significant loss of H3.3 specifically at the telomere. However, SMARCAL1 loss did not significantly change H3.3 incorporation at either telomeric chromatin or in Alu repeats, which are interspersed throughout the genome and here used as a nonspecific repetitive element control (Figure 4). If anything, SMARCAL1 depletion led to a slight increase in chromatin-bound H3.3—the opposite of a phenocopy of ATRX/DAXX loss.

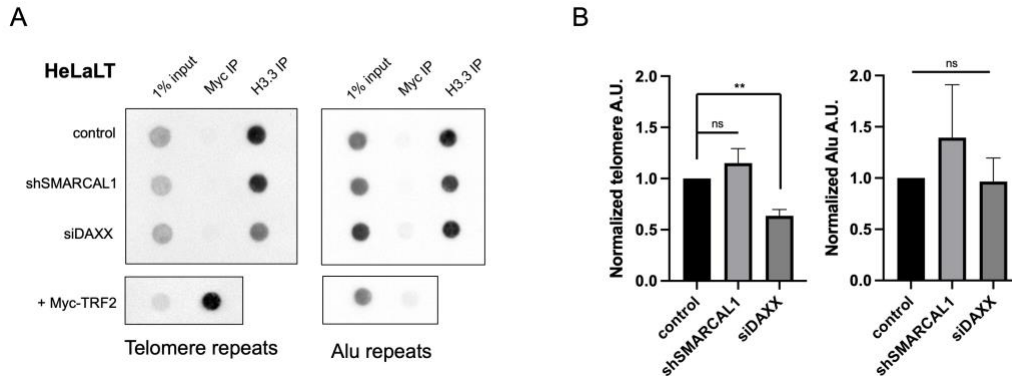


**Figure 4: SMARCAL1 depletion does not affect H3.3 incorporation at telomeres.**

- A. Representative southern dot blots of H3.3 ChIP experiments performed in HeLaLT cells. Cells were either incubated with doxycycline-containing media to induce SMARCAL1 knockdown for 6 days, or transfected on days 0 and 3 with an siRNA against DAXX before collection on day 6. Inputs represent 1% of total chromatin. Myc IP was used as a negative control (top) or positive control in cells expressing Myc-tagged TRF2 (bottom). Probing for Alu repeats served as a negative control for telomere-binding proteins (TRF2). Chromatin was collected from cells expressing Myc-TRF2 72 hours after transfection.
- B. Quantification of data in A. IP intensity was normalized to 1% input to determine total percentage of H3.3-bound chromatin; this was then normalized to untreated control. Bars represent mean with standard deviation for three biological replicates. \*\*  $p < 0.01$ , ordinary one-way ANOVA with Tukey's multiple comparisons testing.

#### *SMARCAL1 loss changes H3K9 trimethylation at telomeres*

Given that the mechanism of ALT repression by SMARCAL1 did not appear to be driven by histone variant deposition, we asked if it could be occurring at the level of histone modifications. Although there is some debate as to the exact state of chromatin compaction at telomeres in general<sup>[118]</sup>, recent evidence suggests that most telomeres are enriched for euchromatic markers like H4K20 methylation and H3K27 acetylation. ALT telomeres, however, display enrichment of heterochromatin marker H3K9 trimethylation (H3K9me3)<sup>[119]</sup>. Methylation at this residue is mediated by the redundant

methyltransferases suppression of variegation 3-9 homologs 1 and 2 (SUV39H) at the pericentromeric region, but at the telomere is mediated by SET domain bifurcated histone lysine methyltransferase 1 (SETDB1). It has recently been argued that excessive heterochromatinization of the telomere by SETDB1-mediated methylation actually drives emergence of ALT phenotypes<sup>[120]</sup>. We therefore performed ChIP for H3K9me3 to determine if loss of SMARCAL1 affected heterochromatin formation at the telomere.

We found that SMARCAL1 depletion for five days led to a significant decrease in methylation at this residue in HeLaLT cells, to approximately the same extent as depletion of ATRX or SETDB1 over the same amount of time. This was evident not only at the telomere, but at interspersed Alu repeats as well (Figure 5 A-B). The decrease in H3K9me3 observed with ATRX knockdown is likely the result of loss of H3.3, as most telomeric H3K9me3 occurs at this variant as opposed to H3.1/2<sup>[121]</sup>. The fact that SMARCAL1 loss changed the chromatin landscape in a way that seemed to mimic ATRX loss indicated a possible mechanism by which SMARCAL1 depletion could lead to induction of ALT. While ATRX maintains chromatin at the level of histone variant deposition, SMARCAL1 instead maintains histone modification.

We therefore asked what would happen in an ALT cell line, which perhaps was already deficient in telomeric H3K9me3, wondering if additional loss of SMARCAL1 would lead to additional and perhaps unsustainable H3K9me3 depletion. However, when we repeated this experiment in the ALT-positive, ATRX-null cell line VA13, we observed an increase in H3K9me3 at the telomere with SMARCAL1 knockdown, albeit insignificant (Figure 5 C-D). Oddly, we also did not observe a decrease in H3K9me3 with

SETDB1 knockdown in VA13 cells. Possibly, these cells, having no ATRX, already display compromised methylation of H3K9 at telomeres, so any additional decrease is not readily detectable by ChIP. They also may require less SETDB1 to maintain baseline H3K9me3, and our incomplete knockdown was not sufficient for a detectable effect; SETDB1 knockout would yield more conclusive results. We were also limited by timeframe for this experiment, as VA13 cells begin to exhibit significant viability defects within 72 hours of SMARCAL1 knockdown, so it is possible that longer SETDB1 or SMARCAL1 depletion would eventually lead to loss of H3K9me3 in this cell line as well.

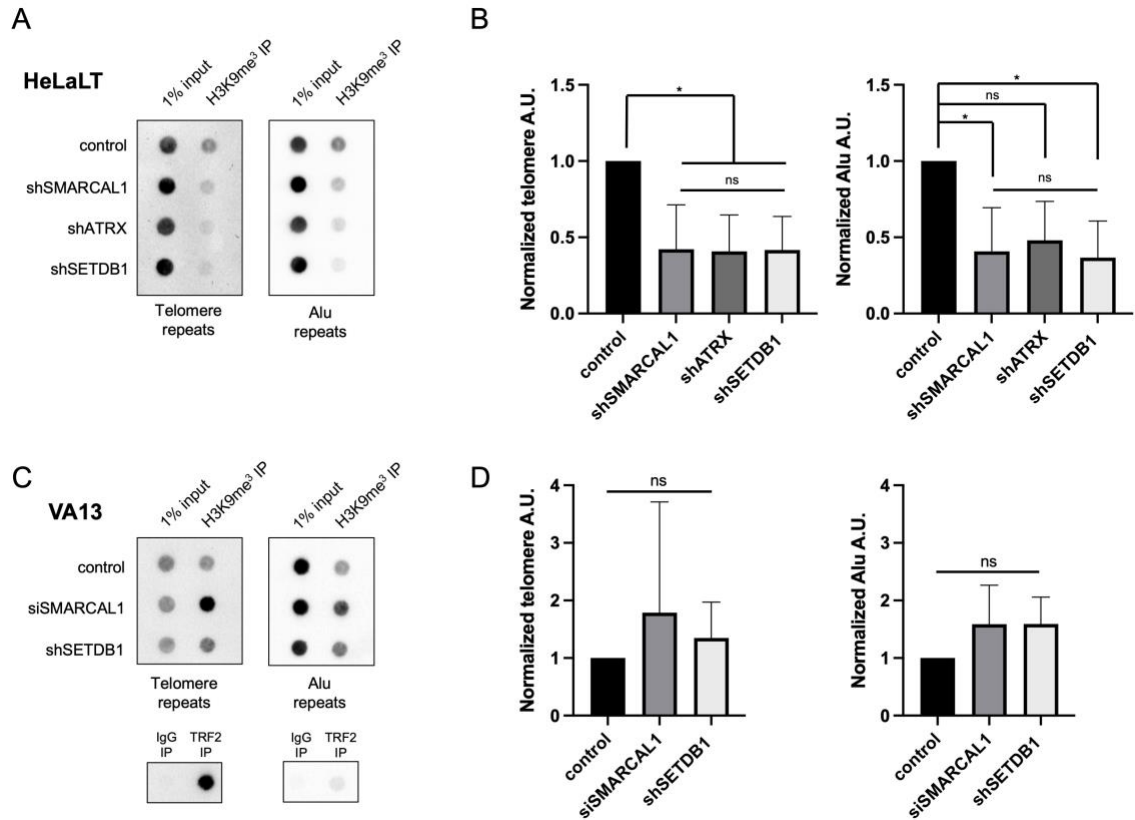


**Figure 5: SMARCAL1 depletion leads to changes in H3K9me3**

- A. Representative southern dot blots of H3K9me3 ChIP experiments performed in HeLaLT cells. Chromatin was collected 5 days after addition of doxycycline to media to induce SMARCAL1 knockdown or 5 days after infection with lentivirus (shATRAX and shSETDB1). Inputs represent 1% of total chromatin.
- B. Quantification of data from A. IP signal was normalized to input to determine percentage of bound H3K9me3; this was then normalized to untreated control for each replicate. Bars represent mean with standard deviation of three biological replicates. \*  $p < 0.05$ , ordinary one-way ANOVA with Tukey's multiple comparisons testing.
- C. Representative southern dot blots of H3K9me3 ChIP experiments performed in VA13 cells. Chromatin was collected 3 days after transfection with siSMARCAL1 or infection with shSETDB1. Inputs represent 1% of total chromatin. IgG IP serves as a negative IP control; TRF2 IP is a telomere-specific control.
- D. Quantification of data from D. IP signal was normalized to input to determine percentage of bound H3K9me3; this was then normalized to untreated control for each replicate. Bars represent mean with standard deviation of three biological replicates. Not significant by ordinary one-way ANOVA with Tukey's multiple comparisons testing.

*ALT cells are sensitive to depletion of ATRX and SMARCAL1*

While completing other experiments, we had observed viability defects in ALT-positive, ATRX-deficient cell lines SaOS2 and VA13 upon depletion of SMARCAL1. Additionally, we noticed that, per the Broad Institute's Cancer Dependency Map, the SMARCAL1-deficient chondrosarcoma line CAL78 is highly dependent on DAXX, while most cell lines require neither ATRX nor DAXX for viability. We therefore wondered if, in the absence of SMARCAL1, ALT cells require the ATRX/DAXX complex. To this end, we knocked down ATRX and DAXX in two SMARCAL1-deficient ALT cell lines, CAL78 and NY (osteosarcoma). Depletion of either ATRX or DAXX alone, or the two in combination, resulted in rapid lethality of both cell lines (Figure 6 A). The lack of synergistic effect of combined ATRX and DAXX knockdown indicated that the important role of ATRX in this context likely involves the H3.3 deposition pathway.

We next wondered if all ALT cell lines were sensitive to combined depletion of ATRX and SMARCAL1, and furthermore if this was an ALT-specific sensitivity. Therefore, we assessed viability upon combined depletion of SMARCAL1 and ATRX in a panel of cell lines, using either siRNA or lentiviral-packaged shRNA depending on knockdown efficiency in each cell line. Overall, ALT cells were more sensitive to combined depletion of SMARCAL1 and ATRX than telomerase-positive or EST cells, although this varied markedly between cell lines (Figure 6 B). For select cells, we expanded the knockdown panel to include individual depletion of ATRX, SMARCAL1, or DAXX (Figure 6 C). The cell lines VA13 and GM847, which lack endogenous ATRX,

are sensitive to SMARCAL1 knockdown, but as expected do not exhibit growth defects with loss of DAXX as it acts in the same pathway as ATRX. G292 lacks functional DAXX due to a translocation<sup>[103]</sup>, and oddly is susceptible to both loss of ATRX and SMARCAL1. Although unexpected, this finding is consistent with data from the Broad Institute's Cancer Dependency Map, and possibly indicates that ATRX is fulfilling multiple functions in terms of replication stress response in these cells. Of our two cell lines with unknown ALT-associated mutations (SW13 and SKLU-1), both exhibit viability defects in the setting of SMARCAL1 knockdown, with no synergy seen in the setting of combined depletion of ATRX and SMARCAL1. SKLU-1 appears to be more sensitive to knockdown of ATRX and/or DAXX alone. Of the ALT-negative cell lines (Figure 6 C, bottom row), MG63 and HeLaLT do not exhibit robust growth defects with any combination of knockdown, though HEK293 seem slightly sensitive to combined depletion of ATRX and DAXX or ATRX and SMARCAL1. Notably, the IMR90-derived fibroblast line SW39 was the most susceptible to combined SMARCAL1 and ATRX knockdown of all telomerase-positive cell lines tested and shows similar viability deficits with ATRX depletion alone. Its isogenic ALT line SW26, however, has completely lost expression of endogenous ATRX. Clearly, although these cells were derived simultaneously from the same fibroblast line, they still have variable epigenetic backgrounds that have a strong influence on how they resolve replication stress and manage chromatin maintenance.

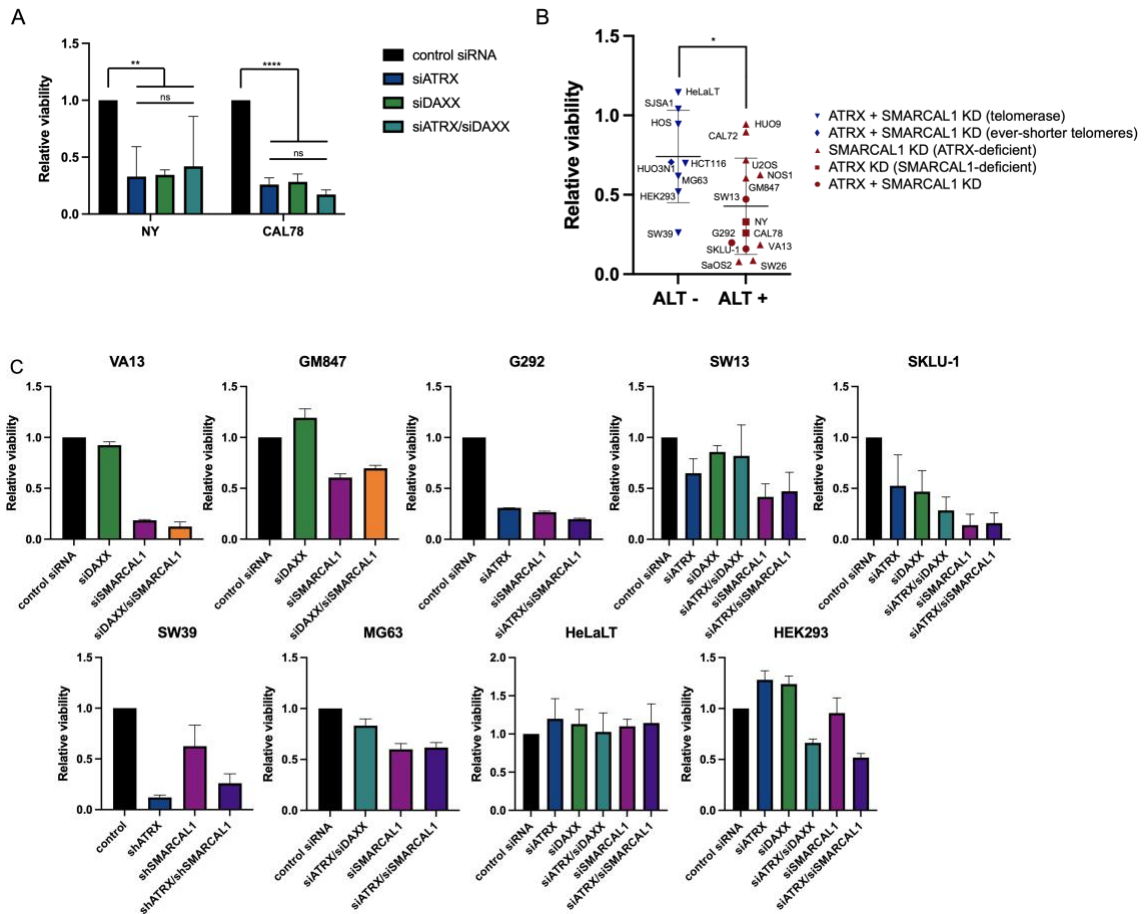


**Figure 6: ALT cells are sensitive to combined depletion of SMARCAL1 and ATRX.**

- A. Relative viability of NY and CAL78 cell lines with knockdown of ATRX and DAXX by luminescence assay. Bars represent mean with standard deviation of six (NY) or three (CAL78) biological replicates. \*\*  $p < 0.01$ , \*\*\*\*  $p < 0.0001$ , ordinary one-way ANOVA with Tukey's multiple comparisons tests.
- B. Relative viability of cell line panel with combined ATRX/SMARCAL1 depletion by RNAi, determined by luminescence assay. Each dot represents mean of at least 3 biological replicates. Bars represent mean for each category with standard deviation.  $p = 0.0308$ , unpaired t test. ALT-negative cell lines: HeLaLT, SJS1, HOS, HCT116, MG63, HEK293, SW39 (telomerase), HUO3N1 (EST). ALT-positive cell lines: HUO9, CAL72, U2OS, NOS1, GM847, VA13, SW26, SaOS2 (ATRX-deficient), NY, CAL78 (SMARCAL1-deficient), SW13, G292, SKLU-1 (WT SMARCAL1 and ATRX).
- C. Expanded relative viability of select cell lines from panel with ATRX, DAXX, and/or SMARCAL1 depletion by RNAi as determined by luminescence assay. Top row represents ALT-positive cell lines, bottom row ALT-negative. Bars represent mean with standard deviation of three biological replicates.

## Discussion

The ALT mechanism of telomere maintenance has long been understood as the result of defects in the ATRX/DAXX H3.3 deposition pathway. However, we are now finding a growing set of ALT-positive tumors wildtype for these proteins but with other mutations, such as loss of SMARCAL1, loss of SLX4IP, or amplification of TOP3A that appear to drive ALT. Here, we have demonstrated that 8 out of 13 tested ALT cell lines cannot tolerate concurrent loss of SMARCAL1 and ATRX (<50% viability), as opposed to 1 out of 8 tested telomerase lines. Others have shown that the ALT-driving TOP3A amplification occurs in a completely mutually exclusive manner with regards to ATRX loss, likely due to insurmountable replication stress that results if both are combined<sup>[101]</sup>. This phenomenon extends to oncogenic mutations not specifically associated with ALT; for example, MYCN amplification is incompatible with ATRX loss due to the extensive DNA damage that results from their combination<sup>[122]</sup>. It therefore seems likely that the lethality we observe with combined depletion of SMARCAL1 and ATRX is the result of the combined replication stress from inefficient fork reversal and loss of H3.3, respectively.

Notably, sensitivity to combined depletion of SMARCAL1 and ATRX varies significantly between cell lines. Our understanding of how the ALT mechanism varies in different types of cancer, and even in the different genetic backgrounds of individual tumors, is currently very poor. Even clonal cell lines derived from the same parent exhibit markedly different replication stress responses<sup>[123]</sup>. We would argue that different susceptibility to loss of SMARCAL1 may represent different degrees or types of

replication stress occurring at the telomere. Chasing down the specific molecular differences that make some ATRX-deficient ALT cells resistant to SMARCAL1 depletion is an important future direction of this project and could lead to a better understanding of the replication stress response that drives ALT in the first place. Our findings are in agreement with a recently-published review article that identified SMARCAL1 as one of the top ALT-specific genetic dependencies based on the Broad Institute's Dependency Map datasets<sup>[55]</sup>.

In looking for a possible mechanism of compensation between ATRX and SMARCAL1, we found that depletion of either leads to changes in H3K9me3 at both the telomeres and interspersed Alu repeats. SMARCAL1 has been primarily studied in the context of stalled fork stabilization; however, being a SNF2 helicase, it potentially has the ability to directly interact with and remodel chromatin. Another possibility is that the accumulation of irreparably stalled telomeric forks in the absence of SMARCAL1 creates a scenario where chromatin cannot be re-compacted after replication, leading to changes in heterochromatic marks like H3K9me3. Regardless, it seems that both ATRX and SMARCAL1 affect chromatin: ATRX functions at the level of histone variant deposition, while SMARCAL1 has no impact on the variant itself, but does play a role in histone modification.

While it is interesting that we observed opposite results in an ALT-positive and an ALT-negative cell line, it is impossible to draw general conclusions about the ALT mechanism from just two cell lines. Future directions for this project will include expanding these experiments to include other cell lines, and determining if this is indeed

a general trend or simply cell type-specific. Also strange is the fact that depletion of SETDB1, considered the primary methylator of H3K9 at the telomere, did not affect presence of H3K9me3 and if anything, increased it in an ALT cell line. While others have shown telomeric dependence on SETDB1 for methylation at this residue, the possibility remains that this is yet another pathway that varies between cell lines.

However, if we consider that loss of SMARCAL1 may be making HeLaLT telomeres more ALT-like, we could form a model in which loss of H3K9me3 due to replication fork stalling leads to chromatin decompaction and a state that is permissive for activation of the ALT pathway. Meanwhile, in VA13 cells, which have been undergoing ALT-mediated telomere extension for many population doublings in culture, may have a completely different response to stalled forks that result from depletion of SMARCAL1.

The ALT-specific lethality from combined depletion of SMARCAL1 and ATRX is likely to simply be the result of excessive accumulation of replication stress at fragile ALT telomeres. Our lab previously showed that ALT cells are unable to resolve stalled replication forks in the absence of SMARCAL1<sup>[74]</sup>, and others have demonstrated that ATRX is also required for efficient DNA replication<sup>[63]</sup>. Additionally, defective heterochromatin formation in the absence of both could potentially lead to genomic instability. Overall, these findings demonstrate another possible way to tip the balance of the ALT mechanism over the edge of manageable replication stress, into a state of telomere dysfunction and cell death.

## **CHAPTER THREE: SMARCAL1 INTERACTS WITH HETEROCHROMATIN MAINTENANCE MACHINERY**

### **Abstract**

The chromatin status of ALT telomeres is poorly understood, with debate as to the extent of heterochromatin and euchromatin-associated histone modifications present. Previously, we had determined that loss of the helicase SMARCAL1 leads to depletion of the heterochromatin marker H3K9me3 from telomerase-positive telomeres. In further exploring the possibility that SMARCAL1 influences telomeric chromatin, we determined that it forms a complex with the histone methyltransferase SETDB1 and interacts directly with the heterochromatin propagator HP1. Furthermore, SMARCAL1 depletion changes the presence of HP1 isoforms at telomeres, with an increase in HP1 $\beta$  and decrease in HP1 $\gamma$ . Although the consequences for heterochromatin maintenance remain unclear, our results indicate a previously undescribed interaction of SMARCAL1 directly with chromatin remodeling machinery.

### **Introduction**

Telomeric chromatin, though generally transcriptionally silent outside the context of ALT, is currently thought to be euchromatic judging by histone modifications, with low levels of H3K9 trimethylation and H4K20 trimethylation<sup>[124–126,119]</sup>, and enrichment of H4K20 methylation and H3K27 acetylation<sup>[119,125]</sup>. ALT telomeres, however, display an increase in heterochromatin mediated by H3K9me3<sup>[119,120,127]</sup>.

It was originally shown that loss of the redundant methyltransferase homologs SUV39H induced activation of ALT phenotypes, and thus it was assumed that loss of histone methylation led to a more open chromatin conformation, which allowed for homologous recombination and therefore ALT activity<sup>[128,129]</sup>. However, it was subsequently demonstrated that SUV39H is absent from telomeres, and telomeric H3K9me3 is actually maintained by another histone methyltransferase, SETDB1. SUV39H depletion leads to ALT phenotypes because it depletes H3K9me3 from the pericentromeric region, displacing the H3K9me3-binding protein HP1 $\alpha$ . The pool of HP1 $\alpha$  then re-localizes to the telomeres, where it propagates SETDB1-mediated H3K9me3 deposition, presumably leading to chromatin compaction that is somehow permissive of ALT<sup>[120]</sup>.

In humans, HP1 has three distinct isoforms— $\alpha$ ,  $\beta$ , and  $\gamma$ . All three act as readers of the H3K9me3 mark, and they have significant overlapping functions, but the unique role of each isoform has not been completely teased apart. For example, HP1 $\alpha$  and HP1 $\beta$  are classically associated with heterochromatin and transcriptional silencing, while HP1 $\gamma$  is found at euchromatic regions and plays a role in transcriptional elongation<sup>[130]</sup>.

The three isoforms are structurally similar—the N-terminus consists of a chromodomain (CD), which recognizes and binds H3K9me3<sup>[131,132]</sup>. The C-terminus contains a chromoshadow domain (CSD), which mediates homo- and heterodimerization, as well as interactions with other proteins. Many of these interactions, including dimerization, occur through a five amino acid consensus motif, PXVXL<sup>[133]</sup>. The CD and CSD are connected by a hinge region (Figure 7 A). In addition to heterochromatin

maintenance, HP1 is also involved in sister chromatid cohesion, chromosome segregation, transcriptional regulation, and DNA damage repair<sup>[130]</sup>.

As detailed in the previous chapter, we discovered that SMARCAL1 depletion decreases H3K9me<sub>3</sub> at telomeres in a telomerase-positive cell line, but marginally increases H3K9me<sub>3</sub> at telomeres in an ALT-positive cell line. We therefore wanted to gain a better understanding of how SMARCAL1 might interact with heterochromatin and its associated factors. We focused this analysis on HP1 after we identified two distinct HP1-interacting PXVXL motifs within the DNA-binding HARP domains of SMARCAL1.

## Materials & Methods

### *Cell Lines and Culture Conditions*

Cells were cultured as described in Chapter 2, with the addition of RPE cells grown in DMEM/F12 with 5% FBS and 1% p/s. The following cell lines were also used for these experiments: HEK293, SaOS2, HeLaLT, VA13.

### *siRNA Transfection*

siRNA transfections were carried out using Lipofectamine RNAiMax (Thermo Fisher) as detailed in Chapter 2. HP1 siRNAs were used at a final concentration of 50 nM each. siRNAs used:

SMARCAL1: Dharmacon custom, targets 3' untranslated region (UUU CAC

AGA GAA AUG CUU AUG CAG GU)

HP1 $\alpha$ : Dharmacon custom (GCU UUG AGA GAG GAC UGG AAC)

HP1 $\beta$ : Dharmacon/Horizon Discovery SMARTPOOL L-009716-00

HP1 $\gamma$ : Dharmacon/Horizon Discovery SMARTPOOL L-010033-00

### *Lentiviral Infection/shRNA-Mediated Knockdown*

Lentiviral infection was carried out as described in Chapter 2. The previously described HeLaLT cells harboring inducible shRNA against SMARCAL1 were also used in these experiments. Knockdown was induced by addition of 2  $\mu$ g/mL doxycycline to media. Plasmids used: shSMARCAL1 (Dharmacon SMARTvector inducible hEF1a-TurboGFP), shSETDB1 (Sigma MISSION TRCN0000276105).

### *Plasmid Overexpression*

Cells were transfected using FuGENE reagent (Promega) as discussed in Chapter 2. All SMARCAL1 constructs have N-terminal S-protein-FLAG-biotin (SFB) tag. HP1 constructs have N-terminal hemagglutinin (HA) tag (Addgene numbers: HP1 $\alpha$  24078, HP1 $\beta$  24079, HP1 $\gamma$  24080).

### *Western Blots*

Western blots were performed as detailed in Chapter 2. Antibodies used: FLAG M2 (diluted 1:1000, Signa Aldrich F1804), GAPDH (diluted 1:1000, Santa Cruz sc-47724), HP1 $\alpha$  (diluted 1:500, Invitrogen PA5-17441), HP1 $\beta$  (diluted 1:500, Santa Cruz sc-517288), HP1 $\gamma$  (diluted 1:500, Santa Cruz sc-398562), SMARCAL1 (diluted 1:250, Santa Cruz sc-376377), HA (diluted 1:1000, Cell Signaling 3724S). SETDB1 (diluted 1:500, proteintech 11231-1-AP),  $\alpha$ -tubulin (diluted 1:1000, Cell Signaling 2125S), H3

(diluted 1:1000, abcam ab1791), p53 (diluted 1:500, Santa Cruz sc-126). Blots were quantified by densitometry using BioRad Image Lab 6.1.

#### *Luminescence-Based Viability Assay*

For rescue experiments in SaOS2, cells were transfected with SFB-tagged SMARCAL1 mutant constructs using FuGENE reagent on day 1 after plating. Endogenous SMARCAL1 was knocked down via siRNA to the 3' untranslated region on day 2 and day 4. When cells reached confluency, 1000 cells per well were transferred to 96-well plates. Three wells for each condition were used per biological replicate. Viability assays were carried out on day 7 using CellTiter-Glo reagent (Promega) per manufacturer instructions.

#### *Immunofluorescence-Fluorescence in situ Hybridization (IF-FISH)*

IF-FISH experiments were carried out as described in Chapter 2. Primary antibodies: SMARCAL1 (diluted 1:250, Santa Cruz sc-376377), FLAG M2 (diluted 1:500, Sigma Aldrich F1804). HA (diluted 1:500, Cell Signaling 2367S and 3724S). Secondary antibodies (all diluted 1:250): Donkey anti-mouse IgG AlexaFluor 488 (Jackson ImmunoResearch or abcam), donkey anti-rabbit IgG AlexaFluor 488 (Jackson). Telomere foci areas were measured and counted using ImageJ.

#### *Chromatin Immunoprecipitation (ChIP)*

ChIP experiments were conducted as described at length in Chapter 2. Antibodies used: HA (Cell Signaling 3724S, 3  $\mu$ L per IP), TRF2 (Bethyl A300-796A, 2  $\mu$ g per IP),

IgG (Diagenode C15410206, 2 µg per IP), SETDB1 (proteintech 11231-1-AP, 5 µg per IP).

### *Immunoprecipitation (IP)*

Cells were collected in PBS, pelleted, and lysed in NETN buffer (100 mM NaCl, 20 mM Tris-HCl pH 8.0, 0.5 mM EDTA, 0.5% NP-40) with PIC (Roche) for 10 minutes on ice. Approximately  $5 \times 10^6$  cells were lysed in 600 µL of NETN for each condition. Lysates were sonicated for 20 seconds at 20% amplitude with probe sonicator, then centrifuged for 10 minutes at high speed, 4C. 1% of lysate was reserved as input and stored at 4C. Protein A beads (NEB or Invitrogen Dynabeads) were washed with PBS-T, then pre-loaded with antibody for 1 hour at 4C (15 µL of beads with 3 µg antibody for each condition). After washing beads again three times with PBS-T and once with NETN, beads were added to lysates and allowed to rock overnight at 4C. Beads were then washed three times with NETN. Beads and input samples were resuspended in NETN with 1X Bolt LDS Sample Buffer (Invitrogen) and boiled for 5 minutes at 95C. DTT was added to 100 mM, and samples were resolved on SDS-PAGE gel for western blot. Antibodies used: SETDB1 (proteintech, 11231-1-AP).

### *Statistical Analysis*

Statistical analysis was carried out in GraphPad Prism, as indicated in figure legends. Two-condition experiments were compared by unpaired t test; those with more than two conditions were compared by one-way ANOVA with appropriate multiple comparisons testing. *P*-values of  $< 0.05$  were considered significant.

## Results

### *SMARCAL1 interacts with heterochromatin protein 1*

We discovered two HP1-interacting PXVXL motifs in SMARCAL1, located within the two HARP domains (Figure 7 B). Combined disruption of conformational flexibility conferred by the proline and the nonpolar pocket centered on valine disrupts PXVXL-HP1 interaction<sup>[134]</sup>, so we created mutant versions of SMARCAL1 in which these one or both motifs were interrupted (P295R/V297D or P390R/V392D). By immunoprecipitation, all three HP1 isoforms interacted with wildtype SMARCAL1 and with a version of SMARCAL1 harboring mutations in a single PXVXL motif. However, disruption of both PXVXL motifs completely disrupted the SMARCAL1-HP1 interaction (Figure 7 C). Given that we had recently shown a loss of H3K9me3 at telomeres in the absence of SMARCAL1, we considered the possibility that a SMARCAL1-HP1 axis may regulate this epigenetic mark at telomeric DNA.

To test whether the HP1-SMARCAL1 interaction was important for viability in ALT cells, we knocked down endogenous SMARCAL1 and overexpressed the double PXVXL mutant in SaOS2 cells, which are extremely sensitive to SMARCAL1 knockdown. As controls, we also expressed a SMARCAL1 mutant with disrupted binding to RPA (R17A/K18A/Q19A), which should not be required for any function at telomeres<sup>[102]</sup>, and an ATPase-dead mutant (R764Q)<sup>[109]</sup>, which we did not expect to rescue SMARCAL1 knockdown-induced lethality as it does not successfully remodel forks.

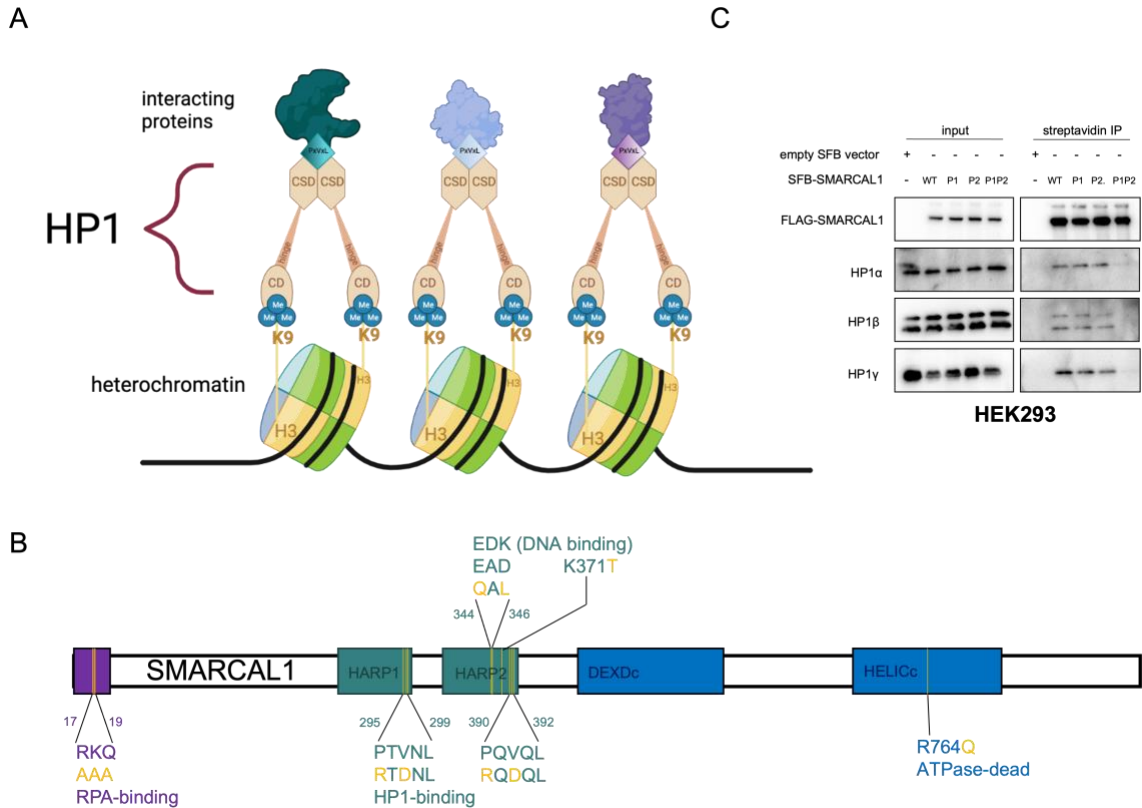


**Figure 7: SMARCAL1 interacts with HP1**

- Schematic of HP1-mediated heterochromatin. HP1 binds to H3K9me3 via its chromodomain (CD). The CD is connected to the chromoshadow domain (CSD) by a hinge region. The CSD mediates dimerization, as well as interaction with chromatin-associated proteins containing PXXVL motifs. Figure created using BioRender.
- Linear protein domain structure of SMARCAL1, with major domains labeled and mutant constructs indicated.
- Western blot showing IP of all three isoforms of HA-tagged HP1 using a streptavidin IP of biotin (SFB)-tagged SMARCAL1 with mutated PXXVL motifs in the HARP1 domain (P1), HARP2 domain (P2) or both (P1P2). This experiment was performed by Himabindu Gali.

Surprisingly, all three mutant versions of SMARCAL1 rescued viability in the setting of endogenous knockdown (Figure 8 A). The HP1-binding mutant did so the least effectively, but also had the poorest overall expression by western blot (Figure 8 B), which is likely confounding.

Mutant forms of SMARCAL1 tend to express variably across cell lines, with the HP1-binding mutant and other HARP domain mutants typically the least robust. This has made it difficult to assess metrics like viability rescue and frequency of co-localization, as it is impossible to compare the mutants to the wildtype protein when they express so poorly. Others have shown that protein expression of SUV39H and SETDB1 is stabilized by interaction with HP1, and that HP1-binding mutant versions of these proteins undergo proteasomal degradation<sup>[135]</sup>. To determine if this was also true for SMARCAL1, we compared wildtype SMARCAL1, the HP1-binding mutant, and another HARP mutant (EDK; E344Q/D346L/K371T)<sup>[136]</sup>, which demonstrates disrupted DNA-binding ability but maintains interaction with HP1. After overexpressing each in untransformed RPE cells, we treated with MG132 proteasome inhibitor for 24 hours and assessed protein stability by western blot (Figure 8 C). In RPE cells, there was notable stabilization of both the PXVXL and EDK mutants with proteasome inhibition, but not the wildtype, indicating that, although not necessarily HP1-specific, displacement of SMARCAL1 from its normal DNA or chromatin interaction leads to proteasomal degradation. This helps to explain some of the difficulties we have had in expressing various mutant versions of SMARCAL1.

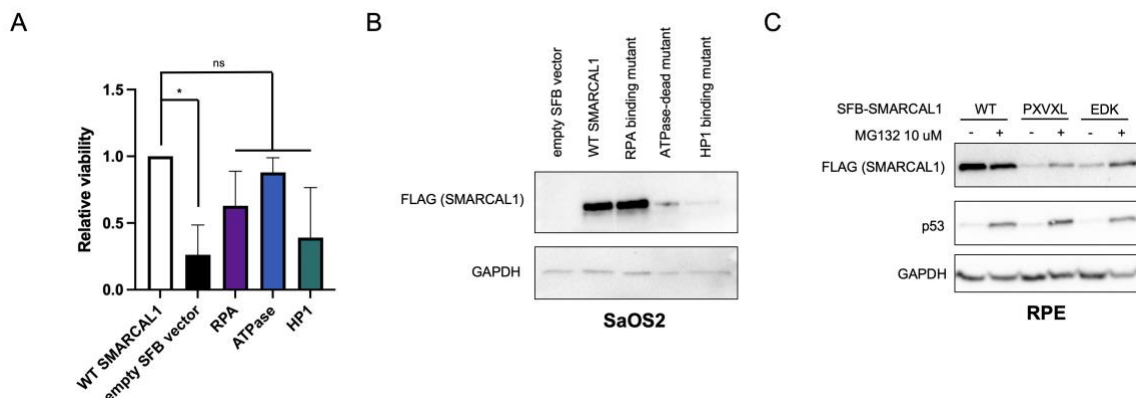


**Figure 8: SMARCAL1 mutants express poorly, but rescue viability in SaOS2.**

- Relative viability by luminescence assay of SaOS2 cells with overexpression of SMARCAL1 mutants after endogenous knockdown. Bars represent mean of three biological replicates with standard deviation. \*  $p < 0.05$ , ordinary one-way ANOVA with Tukey's multiple comparisons testing.
- Representative western blot demonstrating overexpression of SMARCAL1 mutant constructs, 96 hours post-transfection. GAPDH was used as a loading control.
- Western blot demonstrating stabilization of HP1-binding (PXVXL) and DNA-binding (EDK) SMARCAL1 mutants upon proteasome inhibition. Cells were treated with 10  $\mu$ M MG132 for 24 hours prior to lysis. p53 was used as an MG132 control and GAPDH was used as a loading control.

### *HP1 does not recruit SMARCAL1 to telomeres*

Although the SMARCAL1-HP1 interaction appears to be dispensable for survival of ALT cells, we asked if the presence of HP1 at telomeres is what drives SMARCAL1 recruitment. Since the RPA interaction that recruits the helicase to stalled forks elsewhere in the genome does not seem necessary for recruitment to the telomere<sup>[110]</sup>, how SMARCAL1 is recruited to sites of telomeric damage is somewhat of a mystery. To this end, we knocked down all three isoforms of HP1 in SaOS2 cells and performed IF-FISH to look for telomeric localization of SMARCAL1. However, we saw no difference

between mock-transfected cells and HP1 knockdown cells (Figure 9 A-C). Although knockdown of HP1 was incomplete (Figure 9 C), we would expect to see some defect in localization even with partial knockdown if HP1 interaction were driving SMARCAL1 recruitment. Additionally, although expression of the HP1-binding mutant SMARCAL1 was consistently very poor (see Figure 8 B-C), we did observe foci formation in two out of approximately 100 cells counted, and these robustly co-localized with telomeres (Figure 9 D). Although it is difficult to draw concrete conclusions from these experiments, these data do imply that the SMARCAL1-HP1 interaction is not required for the localization of SMARCAL1 to telomeres.

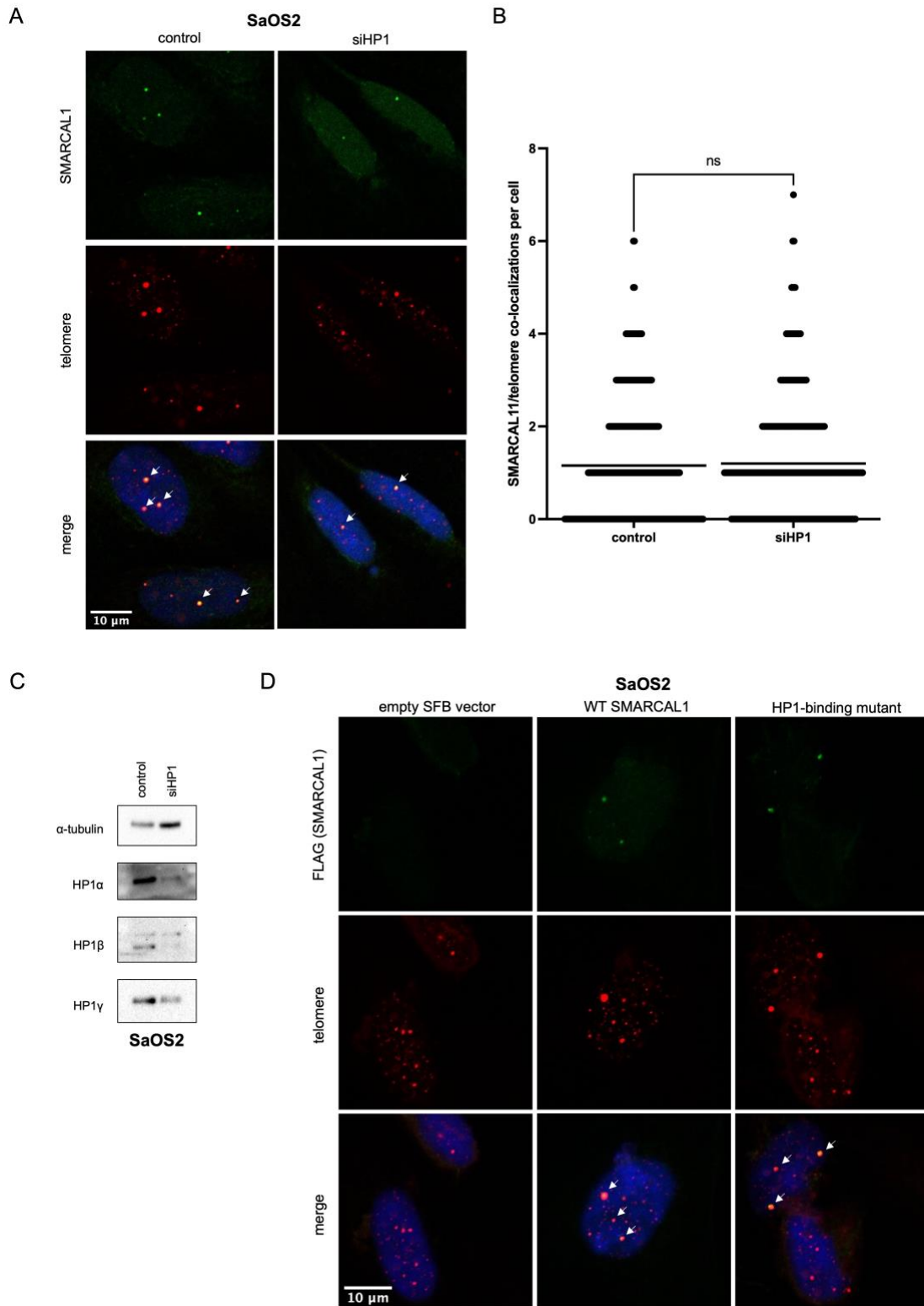


**Figure 9: HP1 does not recruit SMARCAL1 to telomeres.**

- A. Representative IF-FISH images of SaOS2 cells stained for SMARCAL1 (IF) and telomeres (FISH), and counterstained with DAPI. White arrows indicate SMARCAL1 co-localization with telomeres. Cells were treated with siRNA to all three isoforms of HP1 72 hours prior to fixation for staining.
- B. Quantification of data from A. Each dot represents number of SMARCAL1/telomere co-localizations in one cell. Bars represent mean co-localizations per cell from three biological replicates; at least 100 cells were counted per condition per experiment.  $p = 0.6726$ , unpaired t test.
- C. Representative western blot demonstrating HP1 knockdown in SaOS2 cells for IF-FISH experiments.  $\alpha$ -tubulin was used as a loading control.
- D. IF-FISH images of SaOS2 cells overexpressing SFB-tagged WT or PXVXL HP1-binding mutant SMARCAL1 and stained for FLAG (IF) and telomeres (FISH), and counterstained with DAPI. White arrows indicate co-localization of SMARCAL1 and telomeres. Cells were fixed 48 hours after transfection with SFB-tagged SMARCAL1.

*SMARCAL1 depletion changes HP1 localization to telomeres*

Naturally, we then asked if the opposite was true—does SMARCAL1 play a role in the recruitment of HP1 to telomeres? We overexpressed HA-tagged versions of each individual HP1 isoform in ALT-positive VA13 cells and performed IF-FISH to determine frequency of co-localization with telomeres. (Figure 10 A-B). We found that, in the absence of SMARCAL1, there was an increase in telomeric co-localization of HP1 $\beta$ , but a decrease in HP1 $\gamma$ . HP1 $\alpha$  co-localization did not significantly change.

Since there was discrepancy in whether SMARCAL1 loss increases or decreases H3K9me3 at the telomere between an ALT and a non-ALT cell line (see Chapter 2), we wanted to repeat this experiment in telomerase-positive HeLaLT to look for possible differences in HP1 localization. However, unlike in VA13, where HA-HP1 forms robust telomeric foci, IF staining for HA-HP1 in HeLaLT cells was too weak to determine changes in frequency. Instead, we overexpressed HA-tagged versions of each isoform of HP1 in HeLaLT cells with inducible shRNA against SMARCAL1 and performed ChIP

for the HA tag to determine telomeric occupancy in the presence and absence of SMARCAL1 (Figure 10 C-D). The trends in isoform co-localization seen in VA13 were reflected in HA-HP1 occupancy at the telomeres of HeLaLT cells—we observed no change in HP1 $\alpha$ , an increase in HP1 $\beta$ , and a decrease in HP1 $\gamma$ . At Alu repeats, this pattern appears the same, although we immunoprecipitated less HA-HP1 from these regions overall compared to the telomere.

Given that each isoform of HP1 responds differently to SMARCAL1 knockdown, we asked if they might interact differently. Each overexpressed isoform runs at a slightly different size by western blot (Figure 10 E), so it is possible to differentiate between them when they are overexpressed together. To this end, we overexpressed versions of HP1 mutated in the CD region (interrupting association with H3K9me3) or the CSD region (interrupting dimerization and other PXVXL motif interactions) and performed an IP for SFB-tagged SMARCAL1 (Figure 10 F). We observed that CSD interruption disrupted the SMARCAL1 interaction with HP1 $\beta$  and HP1 $\gamma$ , while CD mutation interrupted SMARCAL1 interaction with HP1 $\alpha$  and HP1 $\gamma$ .

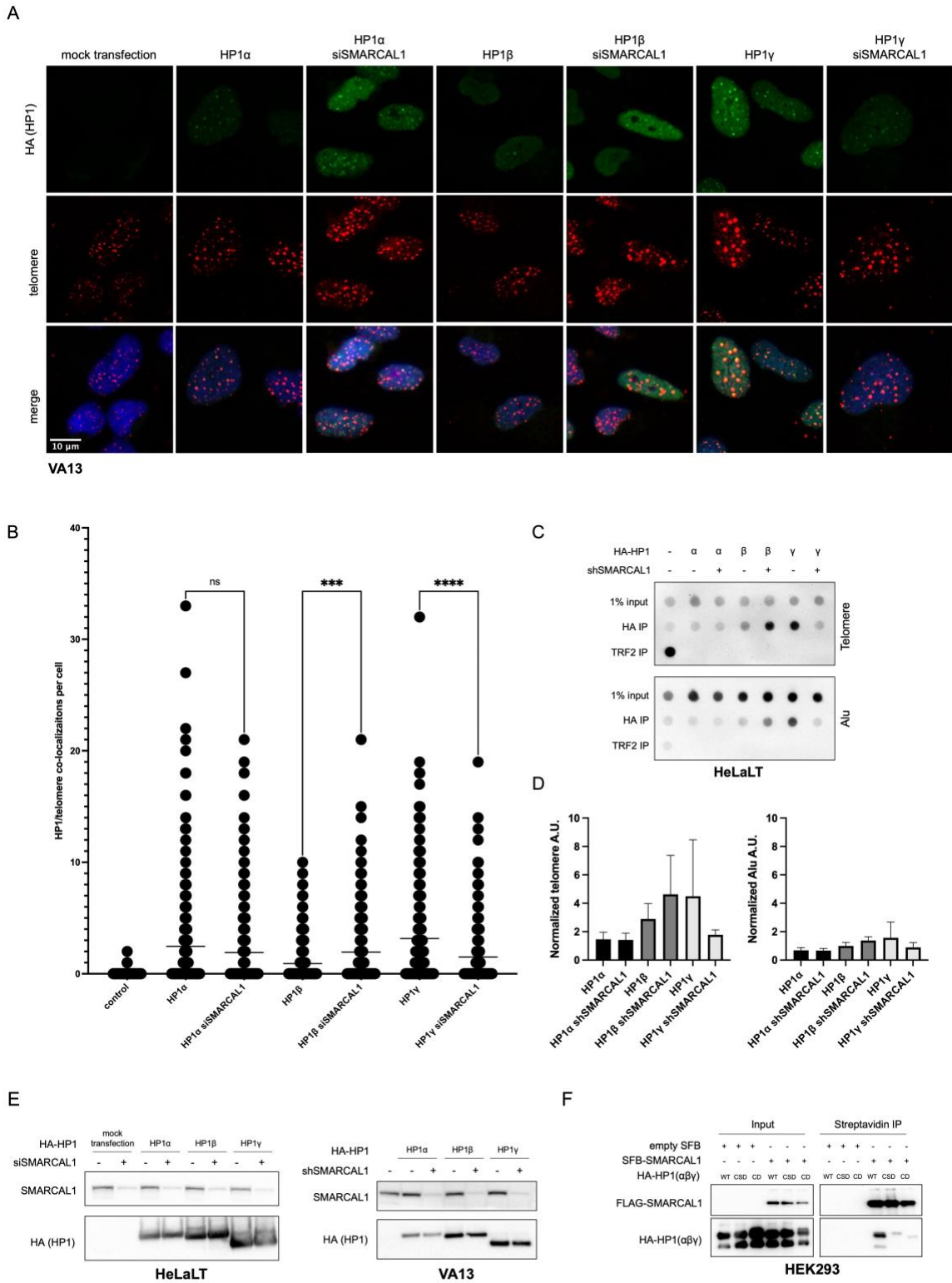


**Figure 10: SMARCAL1 depletion changes HP1 isoform ratios at the telomere.**

- A. Representative IF-FISH images of VA13 cells stained for HA-tagged HP1 (IF) and telomeres (FISH), and counterstained with DAPI. Cells were fixed 72 hours after transfection with HA-tagged HP1 and 48 hours after transfection with siRNA against SMARCAL1.
- B. Quantification of data from A. Each dot represents number of HA-HP1/telomere co-localizations from one cell. At least 100 cells were counted for each condition for each of three biological replicates. Bar represents mean number of co-localizations per cell. \*\*\*  $p < 0.001$ , \*\*\*\*  $p < 0.0001$ , ordinary one-way ANOVA with Tukey's multiple comparisons testing.
- C. Representative southern dot blot from ChIP for HA performed in HeLaLT cells with inducible shRNA against SMARCAL1, overexpressing individual HA-tagged HP1 isoforms. Chromatin was collected 72 hours after transfection with HA-tagged HP1 constructs and 48 hours after induction of shSMARCAL1. Inputs represent 1% of total chromatin. TRF2 IP was performed as positive control for telomeric sequence.
- D. Quantification of data in C. Raw densitometry values were normalized to 1% input to obtain percent occupancy and graphed as fold enrichment over calculated percent occupancy of negative control IP. Bars represent mean of three biological replicates with standard deviation. No significance by ordinary one-way ANOVA with Tukey's multiple comparison's testing.
- E. Representative western blots demonstrating knockdown of SMARCAL1 and overexpression of HA-HP1 in HeLaLT and VA13 cells for these experiments. Pellets were collected at time of chromatin collection (HeLaLT) or immediately prior to fixing and staining (VA13).
- F. HEK293 cells were co-transfected with either empty pDEST-SFB vector or SFB-tagged SMARCAL1 and all three isoforms of HA-tagged HP1. IP for SMARCAL1 was carried out with each mutant version of HP1 using streptavidin-coated magnetic beads. This experiment was performed by Himabindu Gali.

One possible interpretation of this is that those isoforms whose interaction is lost with CD disruption interact with SMARCAL1 only in the setting of heterochromatin, while those lost with CSD disruption are more heavily reliant on interaction with the SMARCAL1 PXVXL motifs. We therefore propose a model in which HP1 $\alpha$  is recruited to telomeres by H3K9me3, regardless of the presence of SMARCAL1; the two form a complex predominantly via association with other chromatin factors. Others have shown that, rather than H3K9me3 in the tail of H3, HP1 $\gamma$  preferentially binds to an interior

globular domain of H3 only available in the presence of SWI/SNF complex chromatin unwinding activity<sup>[137]</sup>. Perhaps SMARCAL1, also a SNF2 helicase, performs the same function at the telomere, and is therefore required for localization of HP1 $\gamma$ . In the absence of SMARCAL1, displacement of HP1 $\gamma$  allows greater telomeric binding by HP1 $\beta$ .

*SMARCAL1 forms a complex with SETDB1*

Given the loss of H3K9me3 in telomerase-positive cell lines with SMARCAL1 knockdown, and the differences in HP1 localization to telomeres seen in both telomerase and ALT-positive cell lines, we wondered if SMARCAL1 loss affected localization of SETDB1, the primary methyltransferase responsible for deposition of H3K9me3 at the telomere. In HeLaLT cells, we knocked down SMARCAL1 and performed ChIP for SETDB1 at telomeres and Alu repeats (Figure 11 A-B). Although our assay was not sensitive enough to detect significant differences, knockdown of SMARCAL1 trends toward decreasing SETDB1 occupancy at telomeres. This is expected based on the loss of telomeric H3K9me3 in these cells, and we remain unable to differentiate whether this is a cause or consequence of SETDB1 loss.

As SMARCAL1 appears to affect SETDB1 localization, we wondered if the two proteins interacted in a complex. Precedent has been set for this interaction, between orthologs SMRC-1 and methyltransferase 2 (MET-2) in *Caenorhabditis elegans*<sup>[138]</sup>. Additionally, we wondered if this interaction was via HP1. We therefore overexpressed either wildtype or PXVXL-mutant SFB-tagged SMARCAL1 in HEK293 cells and performed an immunoprecipitation for SETDB1. We found that both the wildtype and HP1-binding mutant SMARCAL1 did co-immunoprecipitate with SETDB1 (Figure 11 C,

left). Expression of the HP1-binding (PXVXL) mutant was consistently poor, as expected, but when normalized to the total amount expressed in the input, there was no difference in immunoprecipitation efficiency between the wildtype and mutant (Figure 11 D). This interaction was reproducible in ALT-positive VA13 cells as well (Figure 11 C, right). We concluded that the SMARCAL1-SETDB1 interaction exists but is independent of the SMARCAL1 interaction with HP1. Notably, overexpression of either wildtype SMARCAL1 or the mutant did not change SETDB1 association with total H3, which we used as a loading control.

Finally, even though the interaction between SMARCAL1 and HP1 seemed to be unrelated to the interaction between SMARCAL1 and SETDB1, we asked what the functional consequences of loss of SETDB1 would be in an ALT cell line. We had already seen in VA13 that the degree of knockdown we were able to achieve did not seem to affect H3K9me3 at the telomere. However, when we knocked down SETDB1 in SaOS2 cells, we observed strikingly large telomere foci visible by telomere FISH (Figure 11 E-F). Although it is not known exactly what they represent, these telomere dysfunction-induced foci (TIF) are reminiscent of those seen in the setting of SMARCAL1 knockdown. Often, an increase in TIF is considered an escalation of replication stress and ALT activity, indicating that loss of SETDB1 in SaOS2 cells may be driving an increase in telomere dysfunction. This contrasts with what was observed previously in U2OS cells, in which loss of SETDB1 lead to a decrease in APB formation and no apparent emergence of TIF<sup>[120]</sup>. We are unable to explain this discrepancy, except that U2OS and SaOS2 cells, despite both being ALT-positive osteosarcomas, often

behave very differently in culture. For example, SaOS2 are exquisitely dependent on SMARCAL1 for viability, while U2OS can survive without it. In this context, the phenocopy seen with knockdown of SETDB1 and SMARCAL1 specifically in SaOS2 cells supports the idea that heterochromatin formation at the telomere is dependent on both of these proteins, and that they potentially act together in some way.

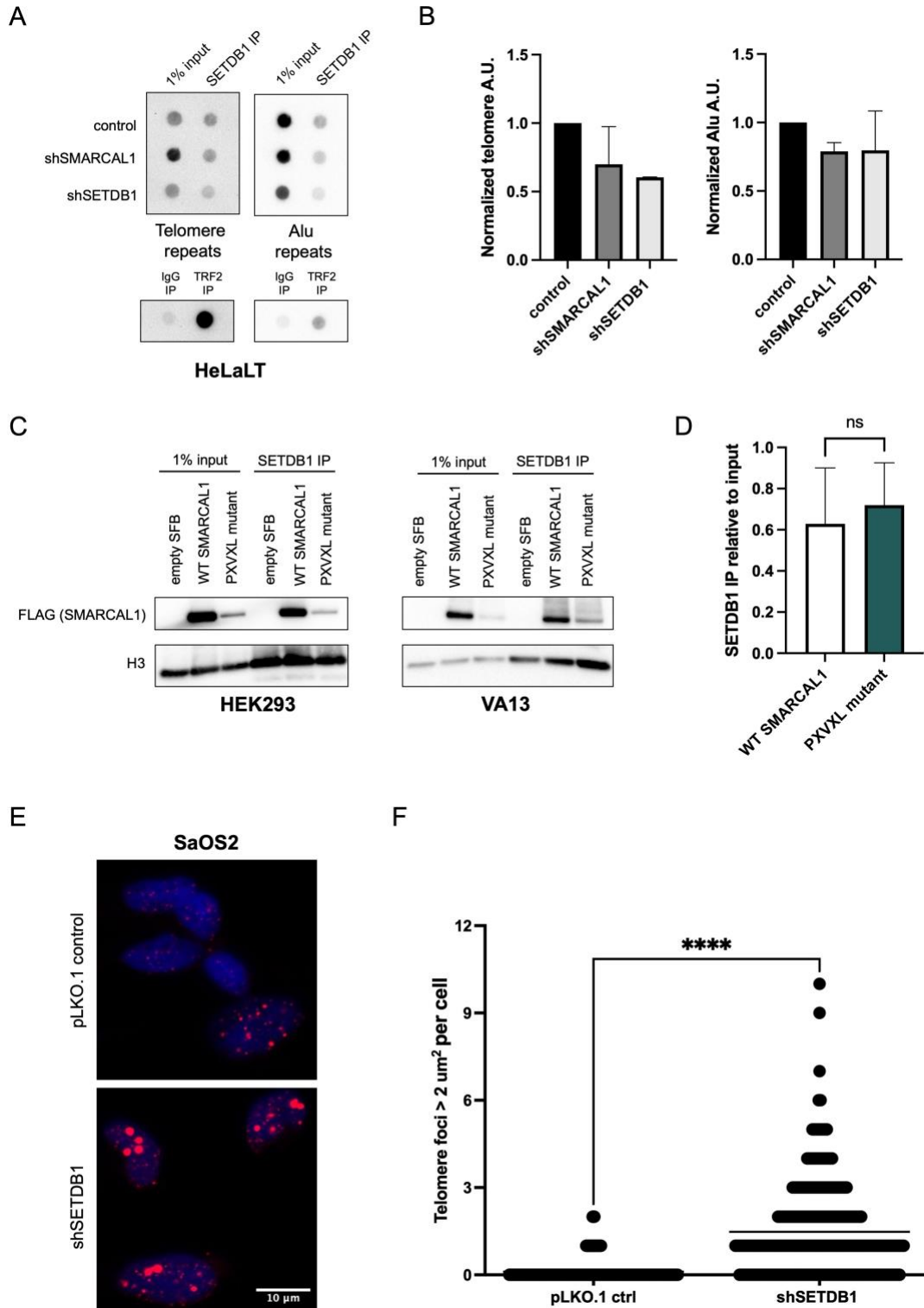


**Figure 11: SMARCAL1 and SETDB1 form a complex and may affect telomeric heterochromatin.**

- A. Representative southern dot blots of SETDB1 ChIP performed in HeLaLT cells. Chromatin was collected 4 days after infection with shSETDB1 or addition of doxycycline to induce shSMARCAL1 expression. IgG IP was used as a negative control, TRF2 IP as a telomere-specific positive control.
- B. Quantification of data in A. IP was normalized to input to obtain percent occupancy of SETDB1; this was then normalized to the untreated control. Bars represent mean with standard deviation of two biological replicates. Not significant by ordinary one-way ANOVA with Tukey's multiple comparisons testing.
- C. Representative western blots of SETDB1 IP experiments. Cells were transfected with empty SFB vector, or SFB-tagged wildtype or HP1-binding (PXVXL) mutant SMARCAL1, 48 hours prior to lysis and IP. Inputs represent 1% of total cell lysate. Total H3 was used as a loading control for both inputs and IPs.
- D. Quantification of data from D. Signal from IP bands was divided by signal from input bands to quantify relative IP signal. Bars represent mean with standard deviation of three biological replicates.  $p = 0.6680$  by unpaired t-test.
- E. Representative images of SaOS2 cells stained for telomeres (FISH) and counterstained with DAPI. Cells were fixed and stained 4 days after infection with shSETDB1 lentivirus or control pLKO.1 vector.
- F. Quantification of data in D. Each dot represents the number of telomere foci with area at least  $2 \mu\text{m}^2$  in one cell. Bar represents mean number of large foci per cell. At least 100 cells were counted per condition for each of 3 biological replicates.  $p < 0.0001$ , unpaired t-test.

## Discussion

Here, we have identified a new complex in human cells, between SMARCAL1, SETDB1, HP1, and histone H3. The SMARCAL1 interaction with HP1 is dependent on two canonical HP1-binding PXVXL motifs, and the interaction is disrupted when both are mutated. The functional consequences of formation and disruption of this complex require further exploration.

Our previous data demonstrated a differential effect on H3K9me3 with SMARCAL1 knockdown between an ALT-positive and ALT-negative cell line, with loss of SMARCAL1 leading to decreased methylation in HeLaLT cells, but a modest increase in methylation in VA13. Given this, we expected to see opposite changes in the

H3K9me3 propagator HP1 at telomeres as well. However, IF-FISH experiments performed in VA13 and ChIP experiments performed in HeLaLT both indicated relatively unchanged HP1 $\alpha$ , an increase in HP1 $\beta$ , and a decrease in HP1 $\gamma$  at telomeres in the absence of SMARCAL1.

Our model of HP1-SMARCAL1 interaction among the different isoforms may help to explain the differential effects on H3K9me3 between ALT and non-ALT cell lines with SMARCAL1 knockdown. HP1 $\alpha$  appears to be recruited regardless of SMARCAL1 presence. As HP1 $\alpha$  is thought to contribute to SETDB1 localization and subsequent H3K9me3 deposition at the telomere, its presence likely varies between cell lines but overall is sufficient to maintain a basal level of heterochromatinization at the telomere. We know comparatively less about the roles of HP1 $\beta$  and HP1 $\gamma$ , particularly as they pertain to propagation of the H3K9me3 mark, and it is possible that they could have different effects depending on the surrounding chromatin landscape and available interacting factors.

We have demonstrated that when SMARCAL1 is depleted, telomeric chromatin undergoes a shift from HP1 $\gamma$  to HP1 $\beta$  occupancy. Previously, it was demonstrated that the opposite—an HP1 $\beta$  to HP1 $\gamma$  switch—occurs upon activation of RNA polymerase II at the long terminal repeat promoter of HIV1<sup>[139]</sup>. Although this has not been studied widely at other inducible promoters, it stands to reason that a  $\gamma$  to  $\beta$  switch may correlate with inactivation of transcription. Although H3K9me3 is typically associated with transcriptional inactivation, ALT is correlated with both higher levels of H3K9me3 and increased telomeric transcription, indicating another case where many other factors are

clearly at play. Additionally, the shelterin component TIN2 interacts strongly with HP1 $\gamma$  and weakly with HP1 $\alpha$  via a PXVXL motif, but not at all with HP1 $\beta$ <sup>[134]</sup>. It is therefore possible that the change from HP1 $\gamma$  to HP1 $\beta$  occupancy at the telomere is also reflective of a change in shelterin-mediated telomere protection, which could contribute to telomere instability. Overall, we conclude that although the exact nature of the interaction between SETDB1, SMARCAL1, and HP1 proved elusive, these three proteins work in tandem to modulate telomeric heterochromatin (Figure 12).

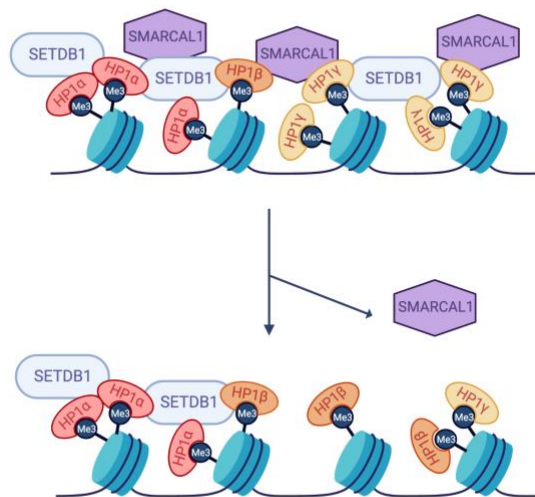


**Figure 12: Hypothetical model demonstrating SMARCAL1 regulation of telomeric chromatin.**

Telomeric H3K9me3 is deposited by SETDB1 and propagated by a feed-forward loop with HP1. SMARCAL1 interacts with both HP1 and SETDB1, forming a key component of telomeric chromatin, particularly in ALT. When SMARCAL1 is depleted, HP1 $\beta$  replaces HP1 $\gamma$  as the dominant isoform present, with no change in HP1 $\alpha$ . In non-ALT cells, SMARCAL1 loss is also accompanied by a decrease in H3K9me3 and a slight decrease in SETDB1. Possible consequences of this include dysregulation of telomeric transcription, chromatin compaction, and recombination, all of which could contribute to development of an ALT-permissive state. Figure created with BioRender.

Furthermore, we have shown that a helicase-dead version of SMARCAL1, which should not be functional, is able to rescue defects in viability seen with knockdown of the endogenous protein. While odd, it was already known that SMARCAL1 functions slightly differently at telomeres, as demonstrated by the lack of RPA-driven recruitment and function. It is possible that the specific fork reversal function perturbed by the R764Q mutation is not needed to compensate for chromatin defects caused by loss of ATRX and persistent telomeric stress. Recently, one group demonstrated that SMARCAL1 was able to anneal single-stranded DNA in the absence of ATP and confirmed annealing activity in a helicase-dead mutant. They further demonstrated that SMARCAL1 was able to anneal single-stranded DNA in the absence of RPA<sup>[140]</sup>. This provides further evidence that SMARCAL1 may remodel DNA in multiple ways, not just via ATPase-dependent annealing of RPA-coated strands. Overall, our findings and those of others indicate that the formation and resolution of specific replication stress-induced DNA structures that form at telomeres merit further investigation.

## CHAPTER FOUR: FINAL THOUGHTS AND FUTURE DIRECTIONS

### Summary

A major finding of this work is that loss of SMARCAL1 does not directly phenocopy loss of the ATRX/DAXX complex by disrupting histone H3.3 deposition at the telomere, but does lead to decreased H3K9me3 at non-ALT telomeres. This indicates a possible mechanism by which SMARCAL1 depletion could contribute to the induction of ALT, disrupting telomeric heterochromatin similarly to depletion of ATRX. However, our results indicate that once the ALT mechanism is activated, SMARCAL1 is no longer required to maintain telomeric heterochromatin, as seen in the ATRX-deficient VA13 line. Additionally, we have shown that ALT-positive cell lines are more susceptible to combined depletion of ATRX and SMARCAL1 than their telomerase-positive counterparts. Although it seems likely that this partial synthetic lethality has more to do with accumulation of an overall unmanageable level of replication stress than any real overlap in direct function, this still represents a potentially targetable susceptibility of ALT cancers.

Additionally, we have identified a novel complex for SMARCAL1, which includes the histone methyltransferase SETDB1, the heterochromatin propagator HP1, and histone H3. SMARCAL1 interacts with HP1 via two PXVXL motifs, and this interaction prevents proteasomal degradation of SMARCAL1. The SMARCAL1-SETDB1 interaction seems to be independent of the SMARCAL1-HP1 interaction.

We were unable to determine the exact order of recruitment of this complex to chromatin, but SMARCAL1 depletion results in a shift of telomeric HP1 occupancy from

the  $\gamma$  to  $\beta$  isoforms by two different assays, in two different cell lines. Based on what is known about the differences between isoforms, a  $\gamma$  to  $\beta$  shift likely represents change from a more euchromatic to heterochromatic state.

SETDB1 loss in an ALT cell line appears to drive telomere clustering and TIF formation, similarly to SMARCAL1 loss. We saw a subtle decrease in SETDB1 localization to telomeres in the absence of SMARCAL1, but likely not enough to explain the striking increase in telomeric size observed by FISH. However, this does imply that in some way, SMARCAL1 and SETDB1 are functioning in the same axis. Overall, the exact contribution of any of these proteins to heterochromatin formation and maintenance likely varies based on the genetic and epigenetic backgrounds of each cell line.

### **Future Directions**

First, we noticed that although ALT cells overall were highly sensitive to combined depletion of SMARCAL1 and ATRX, there were several osteosarcoma lines (CAL72, HUO9, U2OS, and NOS1) that did not fit this pattern. This led us to question if these cell lines experienced less overall replication stress at telomeres, or perhaps just a different form of replication stress. An intriguing possibility is that these cell lines may experience predominantly lagging strand damage; SMARCAL1, which responds predominantly to leading-strand damage<sup>[140]</sup>, would thus not be helpful. This could be assessed by a combination of chromosome-orientation FISH, which allows for differentiation of the leading and lagging strands in metaphase spreads, and IF staining for DNA damage markers such as  $\gamma$ H2AX.

The findings related to H3K9me3 ChIP merit repeating in an array of telomerase and ALT-positive cell lines. Although still an imperfect system, using a panel of cells would give us a better idea of whether the role of SMARCAL1 in heterochromatin maintenance truly diverges by telomere maintenance mechanism, or is something that varies between tissue of origin or some other factor.

Furthermore, the nature of the SMARCAL1-HP1-SETDB1 complex requires further exploration. Although we did not see gross defects in SMARCAL1 localization to telomeres with partial knockdown of all HP1 isoforms, it might be worth complete knockout of each individually. This would help determine the validity of our model, which leaves room for partial telomeric recruitment of SMARCAL1 by HP1 $\alpha$ .

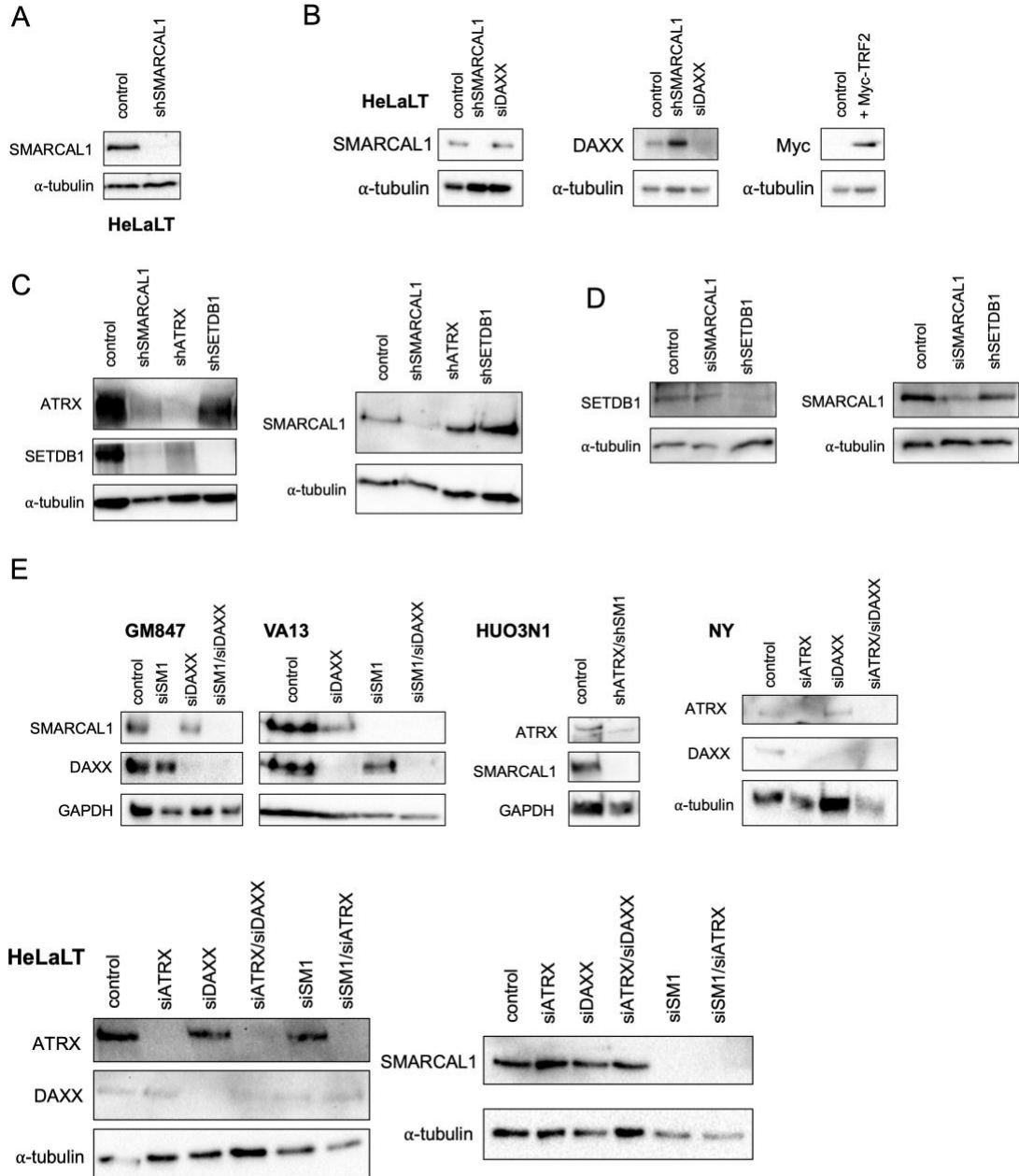
Our inability to express the HP1-binding mutant is frustrating, but may in and of itself be an interesting result. Based on several years of highly inconsistent mutant expression, it seems that those with the strongest expression may be mutated in domains that are least important for cellular function. A CRISPR tiling screen could potentially define this more clearly. By creating mutations along the entire protein, crucial domains can be identified as those with the highest dropout rate among in-frame indels<sup>[141]</sup>. Of particular interest would be domains that are required for ALT cell viability, but not for general protection from DNA damaging agents such as hydroxyurea, which induce genome-wide fork stalling. Based on the findings from our rescue experiments, we are relatively hopeful that these domains exist.

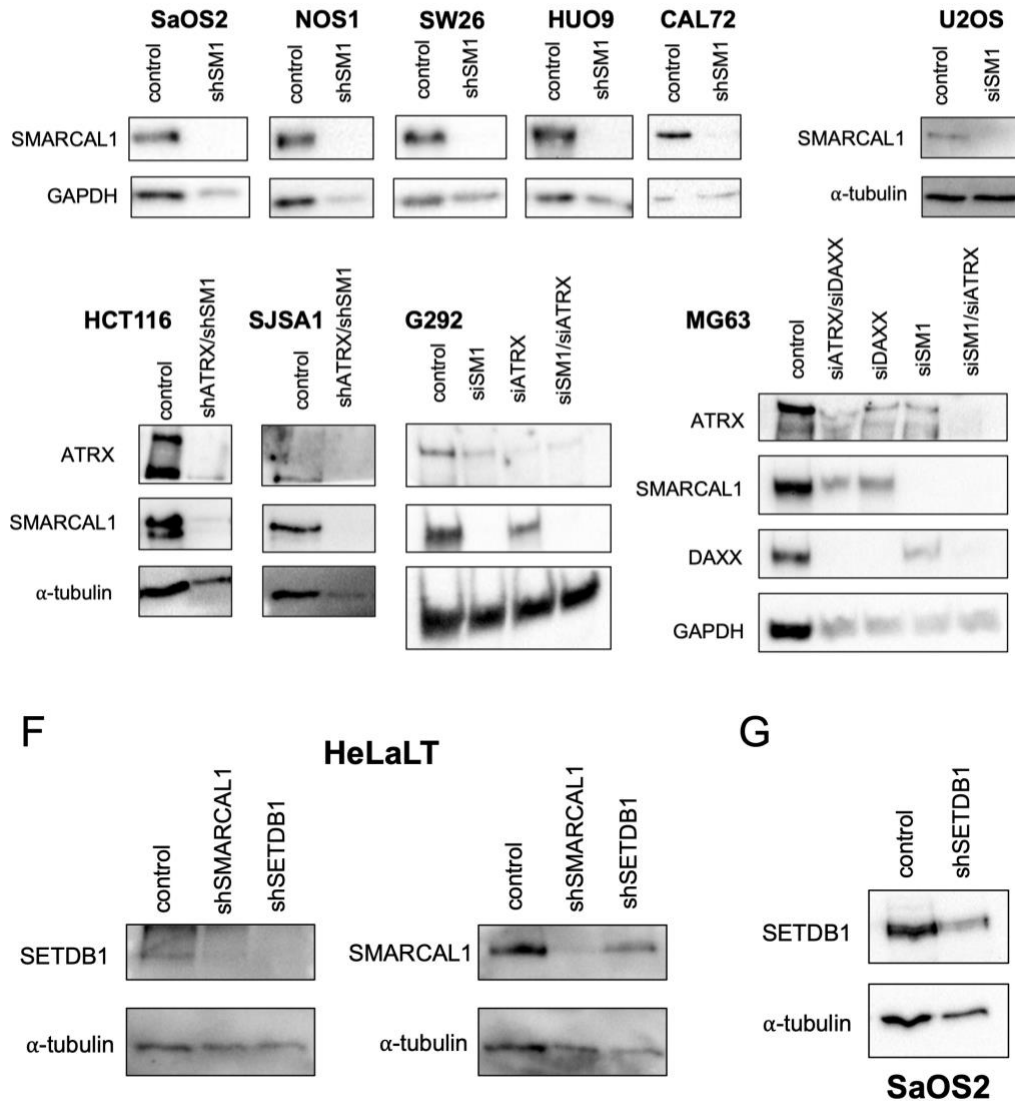
### **Final Thoughts**

This body of work highlights the fact that the alternative lengthening of telomeres cannot be described by one single mechanism. Findings from a single cell line, or even a subset of cell lines, should simply not be used to make broad statements about ALT. As a whole, the field at this point should be trying to understand what makes ALT tumors different from each other, rather than focusing so much on what unites them.

In addition, our research and that of others has highlighted the fact that ALT is a precarious mechanism of telomere elongation. The reliance on chronic replication stress to facilitate telomere elongation puts these cells at a disadvantage when it comes to dealing with any additional DNA damage, whether it is from loss of a compensatory protein or induced by common environmental or chemotherapeutic stresses. Elucidating the subtleties of the ALT mechanism, far down the road, could lead to highly personalized therapies that require lower drug dosages to push these tumors over the brink of unsustainable DNA damage, leading to fewer side effects and hopefully better outcomes.

## APPENDIX





### Supplementary figure: Western blots confirming knockdown

- Representative western blot demonstrating 5-day knockdown of SMARCAL1 by inducible shRNA in HeLaLT for ATRX/telomere IF-FISH experiments (Figure 3).  $\alpha$ -tubulin was used as a loading control.
- Representative western blot demonstrating knockdown of SMARCAL1 (inducible shRNA) or DAXX (siRNA), and overexpression of Myc-TRF2 in HeLaLT cells at time of chromatin collection for H3.3 ChIP experiments (Figure 4).  $\alpha$ -tubulin was used as a loading control.
- Representative western blots demonstrating shRNA-mediated knockdown of ATRX, SETDB1, and SMARCAL1 (inducible) in HeLaLT cells at time of

chromatin collection for H3K9me3 ChIP experiments (Figure 5).  $\alpha$ -tubulin was used as a loading control.

- D. Representative western blots demonstrating knockdown of SETDB1 (shRNA) and SMARCAL1 (siRNA) in VA13 cells at time of chromatin collection in H3K9me3 ChIP experiments (Figure 5).  $\alpha$ -tubulin was used as a loading control.
- E. Representative western blots showing knockdown of ATRX, DAXX, and/or SMARCAL1 (SM1) by lentiviral infection (shATRX), inducible shRNA expression (shSM1), or siRNA for viability assays (Figure 6). GAPDH and  $\alpha$ -tubulin were used as loading controls.
- F. Representative western blots demonstrating SETDB1 and SMARCAL1 knockdown at time of chromatin collection for SETDB1 ChIP experiments (Figure 11).  $\alpha$ -tubulin was used as a loading control.
- G. Representative western blot demonstrating SETDB1 knockdown for FISH experiments (Figure 11). Pellets were collected immediately prior to cell fixation and staining.  $\alpha$ -tubulin was used as a loading control.

## REFERENCES

1. de Lange, T., Shiue, L., Myers, R. M., Cox, D. R., Naylor, S. L., Killery, A. M., & Varmus, H. E. (1990). Structure and variability of human chromosome ends. *Molecular and Cellular Biology*, *10*(2), 518–527. <https://doi.org/10.1128/mcb.10.2.518-527.1990>
2. Makarov, V. L., Hirose, Y., & Langmore, J. P. (1997). Long G Tails at Both Ends of Human Chromosomes Suggest a C Strand Degradation Mechanism for Telomere Shortening. *Cell*, *88*(5), 657–666. [https://doi.org/10.1016/S0092-8674\(00\)81908-X](https://doi.org/10.1016/S0092-8674(00)81908-X)
3. Griffith, J. D., Comeau, L., Rosenfield, S., Stansel, R. M., Bianchi, A., Moss, H., & de Lange, T. (1999). Mammalian Telomeres End in a Large Duplex Loop. *Cell*, *97*(4), 503–514. [https://doi.org/10.1016/S0092-8674\(00\)80760-6](https://doi.org/10.1016/S0092-8674(00)80760-6)
4. Palm, W., & de Lange, T. (2008). How Shelterin Protects Mammalian Telomeres. *Annual Review of Genetics*, *42*(1), 301–334. <https://doi.org/10.1146/annurev.genet.41.110306.130350>
5. Steensel, B. van, Smogorzewska, A., & Lange, T. de. (1998). TRF2 Protects Human Telomeres from End-to-End Fusions. *Cell*, *92*(3), 401–413. [https://doi.org/10.1016/S0092-8674\(00\)80932-0](https://doi.org/10.1016/S0092-8674(00)80932-0)
6. de Lange, T. (2018). Shelterin-Mediated Telomere Protection. *Annual Review of Genetics*, *52*, 223–247. <https://doi.org/10.1146/annurev-genet-032918-021921>
7. Bianchi, A., Smith, S., Chong, L., Elias, P., & de Lange, T. (1997). TRF1 is a dimer and bends telomeric DNA. *The EMBO Journal*, *16*(7), 1785–1794. <https://doi.org/10.1093/emboj/16.7.1785>
8. Broccoli, D., Smogorzewska, A., Chong, L., & de Lange, T. (1997). Human telomeres contain two distinct Myb-related proteins, TRF1 and TRF2. *Nature Genetics*, *17*(2), Article 2. <https://doi.org/10.1038/ng1097-231>
9. Lei, M., Podell, E. R., Baumann, P., & Cech, T. R. (2003). DNA self-recognition in the structure of Pot1 bound to telomeric single-stranded DNA. *Nature*, *426*(6963), Article 6963. <https://doi.org/10.1038/nature02092>
10. Takai, K. K., Kibe, T., Donigian, J. R., Frescas, D., & de Lange, T. (2011). Telomere Protection by TPP1/POT1 Requires Tethering to TIN2. *Molecular Cell*, *44*(4), 647–659. <https://doi.org/10.1016/j.molcel.2011.08.043>

11. Crabbe, L., & Karlseder, J. (2010). Mammalian Rap1 widens its impact. *Nature Cell Biology*, *12*(8), Article 8. <https://doi.org/10.1038/ncb2088>
12. Hayflick, L., & Moorhead, P. S. (1961). The serial cultivation of human diploid cell strains. *Experimental Cell Research*, *25*(3), 585–621. [https://doi.org/10.1016/0014-4827\(61\)90192-6](https://doi.org/10.1016/0014-4827(61)90192-6)
13. Harley, C. B., Futcher, A. B., & Greider, C. W. (1990). Telomeres shorten during ageing of human fibroblasts. *Nature*, *345*(6274), Article 6274. <https://doi.org/10.1038/345458a0>
14. Wynford-Thomas, D., & Kipling, D. (1997). The end-replication problem. *Nature*, *389*(6651), Article 6651. <https://doi.org/10.1038/39210>
15. Sfeir, A. J., Chai, W., Shay, J. W., & Wright, W. E. (2005). Telomere-End Processing: The Terminal Nucleotides of Human Chromosomes. *Molecular Cell*, *18*(1), 131–138. <https://doi.org/10.1016/j.molcel.2005.02.035>
16. Paull, T. T. (2015). Mechanisms of ATM Activation. *Annual Review of Biochemistry*, *84*(1), 711–738. <https://doi.org/10.1146/annurev-biochem-060614-034335>
17. Denchi, E. L., & de Lange, T. (2007). Protection of telomeres through independent control of ATM and ATR by TRF2 and POT1. *Nature*, *448*(7157), Article 7157. <https://doi.org/10.1038/nature06065>
18. Schmutz, I., Timashev, L., Xie, W., Patel, D. J., & de Lange, T. (2017). TRF2 binds branched DNA to safeguard telomere integrity. *Nature Structural & Molecular Biology*, *24*(9), Article 9. <https://doi.org/10.1038/nsmb.3451>
19. Chang, H. H. Y., Pannunzio, N. R., Adachi, N., & Lieber, M. R. (2017). Non-homologous DNA end joining and alternative pathways to double-strand break repair. *Nature Reviews Molecular Cell Biology*, *18*(8), Article 8. <https://doi.org/10.1038/nrm.2017.48>
20. Duursma, A. M., Driscoll, R., Elias, J. E., & Cimprich, K. A. (2013). A Role for the MRN Complex in ATR Activation via TOPBP1 Recruitment. *Molecular Cell*, *50*(1), 116–122. <https://doi.org/10.1016/j.molcel.2013.03.006>
21. Bass, T. E., Luzwick, J. W., Kavanaugh, G., Carroll, C., Dungrawala, H., Glick, G. G., Feldkamp, M. D., Putney, R., Chazin, W. J., & Cortez, D. (2016). ETAA1 acts at stalled replication forks to maintain genome integrity. *Nature Cell Biology*, *18*(11), Article 11. <https://doi.org/10.1038/ncb3415>

22. Gong, Y., & Lange, T. de. (2010). A Shld1-Controlled POT1a Provides Support for Repression of ATR Signaling at Telomeres through RPA Exclusion. *Molecular Cell*, 40(3), 377–387. <https://doi.org/10.1016/j.molcel.2010.10.016>
23. Blackford, A. N., & Jackson, S. P. (2017). ATM, ATR, and DNA-PK: The Trinity at the Heart of the DNA Damage Response. *Molecular Cell*, 66(6), 801–817. <https://doi.org/10.1016/j.molcel.2017.05.015>
24. Fagagna, F. d'Adda di, Reaper, P. M., Clay-Farrace, L., Fiegler, H., Carr, P., von Zglinicki, T., Saretzki, G., Carter, N. P., & Jackson, S. P. (2003). A DNA damage checkpoint response in telomere-initiated senescence. *Nature*, 426(6963), Article 6963. <https://doi.org/10.1038/nature02118>
25. Zglinicki, T. von, Saretzki, G., Ladhoff, J., Fagagna, F. d'Adda di, & Jackson, S. P. (2005). Human cell senescence as a DNA damage response. *Mechanisms of Ageing and Development*, 126(1), 111–117. <https://doi.org/10.1016/j.mad.2004.09.034>
26. Hanahan, D., & Weinberg, R. A. (2000). The Hallmarks of Cancer. *Cell*, 100(1), 57–70. [https://doi.org/10.1016/S0092-8674\(00\)81683-9](https://doi.org/10.1016/S0092-8674(00)81683-9)
27. Maciejowski, J., Li, Y., Bosco, N., Campbell, P. J., & de Lange, T. (2015). Chromothripsis and Kataegis Induced by Telomere Crisis. *Cell*, 163(7), 1641–1654. <https://doi.org/10.1016/j.cell.2015.11.054>
28. Wright, W. E., Pereira-Smith, O. M., & Shay, J. W. (1989). Reversible cellular senescence: Implications for immortalization of normal human diploid fibroblasts. *Molecular and Cellular Biology*, 9(7), 3088–3092. <https://doi.org/10.1128/mcb.9.7.3088-3092.1989>
29. Kim, N. W., Piatyszek, M. A., Prowse, K. R., Harley, C. B., West, M. D., Ho, P. L. C., Coviello, G. M., Wright, W. E., Weinrich, S. L., & Shay, J. W. (1994). Specific Association of Human Telomerase Activity with Immortal Cells and Cancer. *Science*, 266(5193), 2011–2015. <https://doi.org/10.1126/science.7605428>
30. Greider, C. W., & Blackburn, E. H. (1985). Identification of a specific telomere terminal transferase activity in tetrahymena extracts. *Cell*, 43(2, Part 1), 405–413. [https://doi.org/10.1016/0092-8674\(85\)90170-9](https://doi.org/10.1016/0092-8674(85)90170-9)
31. Wright, W. E., Piatyszek, M. A., Rainey, W. E., Byrd, W., & Shay, J. W. (1996). Telomerase activity in human germline and embryonic tissues and cells. *Developmental Genetics*, 18(2), 173–179. [https://doi.org/10.1002/\(SICI\)1520-6408\(1996\)18:2<173::AID-DVG10>3.0.CO;2-3](https://doi.org/10.1002/(SICI)1520-6408(1996)18:2<173::AID-DVG10>3.0.CO;2-3)

32. Feng, J., Funk, W. D., Wang, S.-S., Weinrich, S. L., Avilion, A. A., Chiu, C.-P., Adams, R. R., Chang, E., Allsopp, R. C., Yu, J., Le, S., West, M. D., Harley, C. B., Andrews, W. H., Greider, C. W., & Villeponteau, B. (1995). The RNA Component of Human Telomerase. *Science*, *269*(5228), 1236–1241. <https://doi.org/10.1126/science.7544491>
33. Kolquist, K. A., Ellisen, L. W., Counter, C. M., Meyerson, M. M., Tan, L. K., Weinberg, R. A., Haber, D. A., & Gerald, W. L. (1998). Expression of TERT in early premalignant lesions and a subset of cells in normal tissues. *Nature Genetics*, *19*(2), Article 2. <https://doi.org/10.1038/554>
34. Shay, J. W., & Wright, W. E. (2019). Telomeres and telomerase: Three decades of progress. *Nature Reviews Genetics*, *20*(5), Article 5. <https://doi.org/10.1038/s41576-019-0099-1>
35. Chiba, K., Lorbeer, F. K., Shain, A. H., McSwiggen, D. T., Schruf, E., Oh, A., Ryu, J., Darzacq, X., Bastian, B. C., & Hockemeyer, D. (2017). Mutations in the promoter of the telomerase gene TERT contribute to tumorigenesis by a two-step mechanism. *Science*, *357*(6358), 1416–1420. <https://doi.org/10.1126/science.aao0535>
36. Bryan, T. M., Englezou, A., Gupta, J., Bacchetti, S., & Reddel, R. R. (1995). Telomere elongation in immortal human cells without detectable telomerase activity. *The EMBO Journal*, *14*(17), 4240–4248. <https://doi.org/10.1002/j.1460-2075.1995.tb00098.x>
37. Heaphy, C. M., Subhawong, A. P., Hong, S.-M., Goggins, M. G., Montgomery, E. A., Gabrielson, E., Netto, G. J., Epstein, J. I., Lotan, T. L., Westra, W. H., Shih, I.-M., Iacobuzio-Donahue, C. A., Maitra, A., Li, Q. K., Eberhart, C. G., Taube, J. M., Rakheja, D., Kurman, R. J., Wu, T. C., ... Meeker, A. K. (2011). Prevalence of the Alternative Lengthening of Telomeres Telomere Maintenance Mechanism in Human Cancer Subtypes. *The American Journal of Pathology*, *179*(4), 1608–1615. <https://doi.org/10.1016/j.ajpath.2011.06.018>
38. Roumelioti, F.-M., Sotiriou, S. K., Katsini, V., Chiourea, M., Halazonetis, T. D., & Gagos, S. (2016). Alternative lengthening of human telomeres is a conservative DNA replication process with features of break-induced replication. *EMBO Reports*, *17*(12), 1731–1737. <https://doi.org/10.15252/embr.201643169>
39. Sakofsky, C. J., & Malkova, A. (2017). Break induced replication in eukaryotes: Mechanisms, functions, and consequences. *Critical Reviews in Biochemistry and Molecular Biology*, *52*(4), 395–413. <https://doi.org/10.1080/10409238.2017.1314444>

40. Dilley, R. L., Verma, P., Cho, N. W., Winters, H. D., Wondisford, A. R., & Greenberg, R. A. (2016). Break-induced telomere synthesis underlies alternative telomere maintenance. *Nature*, *539*(7627), Article 7627.  
<https://doi.org/10.1038/nature20099>
41. Flynn, R. L., & Heaphy, C. M. (2019). Surviving Telomere Attrition with the MiDAS Touch. *Trends in Genetics*, *35*(11), 783–785.  
<https://doi.org/10.1016/j.tig.2019.08.008>
42. Min, J., Wright, W. E., & Shay, J. W. (2017). Alternative Lengthening of Telomeres Mediated by Mitotic DNA Synthesis Engages Break-Induced Replication Processes. *Molecular and Cellular Biology*, *37*(20), e00226-17.  
<https://doi.org/10.1128/MCB.00226-17>
43. Min, J., Wright, W. E., & Shay, J. W. (2019). Clustered telomeres in phase-separated nuclear condensates engage mitotic DNA synthesis through BLM and RAD52. *Genes & Development*, *33*(13–14), 814–827.  
<https://doi.org/10.1101/gad.324905.119>
44. Mocanu, C., Karanika, E., Fernández-Casañas, M., Herbert, A., Olukoga, T., Özgürses, M. E., & Chan, K.-L. (2022). DNA replication is highly resilient and persistent under the challenge of mild replication stress. *Cell Reports*, *39*(3), 110701. <https://doi.org/10.1016/j.celrep.2022.110701>
45. Dagg, R. A., Pickett, H. A., Neumann, A. A., Napier, C. E., Henson, J. D., Teber, E. T., Arthur, J. W., Reynolds, C. P., Murray, J., Haber, M., Sobinoff, A. P., Lau, L. M. S., & Reddel, R. R. (2017). Extensive Proliferation of Human Cancer Cells with Ever-Shorter Telomeres. *Cell Reports*, *19*(12), 2544–2556.  
<https://doi.org/10.1016/j.celrep.2017.05.087>
46. Viceconte, N., Dheur, M.-S., Majerova, E., Pierreux, C. E., Baurain, J.-F., van Baren, N., & Decottignies, A. (2017). Highly Aggressive Metastatic Melanoma Cells Unable to Maintain Telomere Length. *Cell Reports*, *19*(12), 2529–2543.  
<https://doi.org/10.1016/j.celrep.2017.05.046>
47. Barthel, F. P., Wei, W., Tang, M., Martinez-Ledesma, E., Hu, X., Amin, S. B., Akdemir, K. C., Seth, S., Song, X., Wang, Q., Lichtenberg, T., Hu, J., Zhang, J., Zheng, S., & Verhaak, R. G. W. (2017). Systematic analysis of telomere length and somatic alterations in 31 cancer types. *Nature Genetics*, *49*(3), Article 3.  
<https://doi.org/10.1038/ng.3781>
48. Claude, E., & Decottignies, A. (2020). Telomere maintenance mechanisms in cancer: Telomerase, ALT or lack thereof. *Current Opinion in Genetics & Development*, *60*, 1–8. <https://doi.org/10.1016/j.gde.2020.01.002>

49. Mason-Osann, E., Gali, H., & Flynn, R. L. (2019). Resolving Roadblocks to Telomere Replication. In L. Balakrishnan & J. A. Stewart (Eds.), *DNA Repair: Methods and Protocols* (pp. 31–57). Springer. [https://doi.org/10.1007/978-1-4939-9500-4\\_2](https://doi.org/10.1007/978-1-4939-9500-4_2)
50. Mondello, C., Pirzio, L., Azzalin, C. M., & Giulotto, E. (2000). Instability of Interstitial Telomeric Sequences in the Human Genome. *Genomics*, *68*(2), 111–117. <https://doi.org/10.1006/geno.2000.6280>
51. Lipps, H. J., & Rhodes, D. (2009). G-quadruplex structures: In vivo evidence and function. *Trends in Cell Biology*, *19*(8), 414–422. <https://doi.org/10.1016/j.tcb.2009.05.002>
52. Vannier, J.-B., Pavicic-Kaltenbrunner, V., Petalcorin, M. I. R., Ding, H., & Boulton, S. J. (2012). RTEL1 Dismantles T Loops and Counteracts Telomeric G4-DNA to Maintain Telomere Integrity. *Cell*, *149*(4), 795–806. <https://doi.org/10.1016/j.cell.2012.03.030>
53. Drosopoulos, W. C., Kosiyatrakul, S. T., Yan, Z., Calderano, S. G., & Schildkraut, C. L. (2012). Human telomeres replicate using chromosome-specific, rather than universal, replication programs. *Journal of Cell Biology*, *197*(2), 253–266. <https://doi.org/10.1083/jcb.201112083>
54. Cesare, A. J., & Reddel, R. R. (2010). Alternative lengthening of telomeres: Models, mechanisms and implications. *Nature Reviews Genetics*, *11*(5), Article 5. <https://doi.org/10.1038/nrg2763>
55. Lu, R., & Pickett, H. A. (2022). Telomeric replication stress: The beginning and the end for alternative lengthening of telomeres cancers. *Open Biology*, *12*(3), 220011. <https://doi.org/10.1098/rsob.220011>
56. Conomos, D., Stutz, M. D., Hills, M., Neumann, A. A., Bryan, T. M., Reddel, R. R., & Pickett, H. A. (2012). Variant repeats are interspersed throughout the telomeres and recruit nuclear receptors in ALT cells. *J Cell Biol*, *199*(6), 893–906. <https://doi.org/10.1083/jcb.201207189>
57. Sfeir, A., Kosiyatrakul, S. T., Hockemeyer, D., MacRae, S. L., Karlseder, J., Schildkraut, C. L., & de Lange, T. (2009). Mammalian Telomeres Resemble Fragile Sites and Require TRF1 for Efficient Replication. *Cell*, *138*(1), 90–103. <https://doi.org/10.1016/j.cell.2009.06.021>
58. Drosopoulos, W. C., Deng, Z., Twayana, S., Kosiyatrakul, S. T., Vladimirova, O., Lieberman, P. M., & Schildkraut, C. L. (2020). TRF2 Mediates Replication

Initiation within Human Telomeres to Prevent Telomere Dysfunction. *Cell Reports*, 33(6), 108379. <https://doi.org/10.1016/j.celrep.2020.108379>

59. Flynn, R. L., Cox, K. E., Jeitany, M., Wakimoto, H., Bryll, A. R., Ganem, N. J., Bersani, F., Pineda, J. R., Suvà, M. L., Benes, C. H., Haber, D. A., Boussin, F. D., & Zou, L. (2015). Alternative Lengthening of Telomeres Renders Cancer Cells Hypersensitive to ATR Inhibitors. *Science (New York, N.Y.)*, 347(6219), 273–277. <https://doi.org/10.1126/science.1257216>
60. Arora, R., Lee, Y., Wischnewski, H., Brun, C. M., Schwarz, T., & Azzalin, C. M. (2014). RNaseH1 regulates TERRA-telomeric DNA hybrids and telomere maintenance in ALT tumour cells. *Nature Communications*, 5(1), Article 1. <https://doi.org/10.1038/ncomms6220>
61. Silva, B., Arora, R., Bione, S., & Azzalin, C. M. (2021). TERRA transcription destabilizes telomere integrity to initiate break-induced replication in human ALT cells. *Nature Communications*, 12(1), Article 1. <https://doi.org/10.1038/s41467-021-24097-6>
62. Heaphy, C. M., de Wilde, R. F., Jiao, Y., Klein, A. P., Edil, B. H., Shi, C., Bettgowda, C., Rodriguez, F. J., Eberhart, C. G., Hebbar, S., Offerhaus, G. J., McLendon, R., Rasheed, B. A., He, Y., Yan, H., Bigner, D. D., Oba-Shinjo, S. M., Marie, S. K. N., Riggins, G. J., ... Meeker, A. K. (2011). Altered Telomeres in Tumors with ATRX and DAXX Mutations. *Science*, 333(6041), 425–425. <https://doi.org/10.1126/science.1207313>
63. Huh, M. S., Ivanochko, D., Hashem, L. E., Curtin, M., Delorme, M., Goodall, E., Yan, K., & Picketts, D. J. (2016). Stalled replication forks within heterochromatin require ATRX for protection. *Cell Death & Disease*, 7(5), Article 5. <https://doi.org/10.1038/cddis.2016.121>
64. Teng, Y.-C., Sundaresan, A., O'Hara, R., Gant, V. U., Li, M., Martire, S., Warshaw, J. N., Basu, A., & Banaszynski, L. A. (2021). ATRX promotes heterochromatin formation to protect cells from G-quadruplex DNA-mediated stress. *Nature Communications*, 12(1), Article 1. <https://doi.org/10.1038/s41467-021-24206-5>
65. Wang, Y., Yang, J., Wild, A. T., Wu, W. H., Shah, R., Danussi, C., Riggins, G. J., Kannan, K., Sulman, E. P., Chan, T. A., & Huse, J. T. (2019). G-quadruplex DNA drives genomic instability and represents a targetable molecular abnormality in ATRX-deficient malignant glioma. *Nature Communications*, 10(1), Article 1. <https://doi.org/10.1038/s41467-019-08905-8>
66. Koschmann, C., Calinescu, A.-A., Nunez, F. J., Mackay, A., Fazal-Salom, J., Thomas, D., Mendez, F., Kamran, N., Dzaman, M., Mulpuri, L., Krasinkiewicz,

- J., Doherty, R., Lemons, R., Brosnan-Cashman, J. A., Li, Y., Roh, S., Zhao, L., Appelman, H., Ferguson, D., ... Castro, M. G. (2016). ATRX loss promotes tumor growth and impairs nonhomologous end joining DNA repair in glioma. *Science Translational Medicine*, 8(328), 328ra28-328ra28. <https://doi.org/10.1126/scitranslmed.aac8228>
67. Juhász, S., Elbakry, A., Mathes, A., & Löbrich, M. (2018). ATRX Promotes DNA Repair Synthesis and Sister Chromatid Exchange during Homologous Recombination. *Molecular Cell*, 71(1), 11-24.e7. <https://doi.org/10.1016/j.molcel.2018.05.014>
68. Pan, X., Chen, Y., Biju, B., Ahmed, N., Kong, J., Goldenberg, M., Huang, J., Mohan, N., Klosek, S., Parsa, K., Guh, C.-Y., Lu, R., Pickett, H. A., Chu, H.-P., & Zhang, D. (2019). FANCM suppresses DNA replication stress at ALT telomeres by disrupting TERRA R-loops. *Scientific Reports*, 9(1), Article 1. <https://doi.org/10.1038/s41598-019-55537-5>
69. Lu, R., O'Rourke, J. J., Sobinoff, A. P., Allen, J. A. M., Nelson, C. B., Tomlinson, C. G., Lee, M., Reddel, R. R., Deans, A. J., & Pickett, H. A. (2019). The FANCM-BLM-TOP3A-RMI complex suppresses alternative lengthening of telomeres (ALT). *Nature Communications*, 10(1), Article 1. <https://doi.org/10.1038/s41467-019-10180-6>
70. Silva, B., Pentz, R., Figueira, A. M., Arora, R., Lee, Y. W., Hodson, C., Wischnewski, H., Deans, A. J., & Azzalin, C. M. (2019). FANCM limits ALT activity by restricting telomeric replication stress induced by deregulated BLM and R-loops. *Nature Communications*, 10(1), Article 1. <https://doi.org/10.1038/s41467-019-10179-z>
71. Fan, Q., Zhang, F., Barrett, B., Ren, K., & Andreassen, P. R. (2009). A role for monoubiquitinated FANCD2 at telomeres in ALT cells. *Nucleic Acids Research*, 37(6), 1740–1754. <https://doi.org/10.1093/nar/gkn995>
72. Saharia, A., & Stewart, S. A. (2009). FEN1 contributes to telomere stability in ALT-positive tumor cells. *Oncogene*, 28(8), Article 8. <https://doi.org/10.1038/onc.2008.458>
73. Zeng, S., Xiang, T., Pandita, T. K., Gonzalez-Suarez, I., Gonzalo, S., Harris, C. C., & Yang, Q. (2009). Telomere recombination requires the MUS81 endonuclease. *Nature Cell Biology*, 11(5), Article 5. <https://doi.org/10.1038/ncb1867>
74. Cox, K. E., Maréchal, A., & Flynn, R. L. (2016). SMARCAL1 Resolves Replication Stress at ALT Telomeres. *Cell Reports*, 14(5), 1032–1040. <https://doi.org/10.1016/j.celrep.2016.01.011>

75. Yeager, T. R., Neumann, A. A., Englezou, A., Huschtscha, L. I., Noble, J. R., & Reddel, R. R. (1999). Telomerase-negative Immortalized Human Cells Contain a Novel Type of Promyelocytic Leukemia (PML) Body1. *Cancer Research*, *59*(17), 4175–4179.
76. Lallemand-Breitenbach, V., & de Thé, H. (2010). PML Nuclear Bodies. *Cold Spring Harbor Perspectives in Biology*, *2*(5), a000661. <https://doi.org/10.1101/cshperspect.a000661>
77. Dickey, J. S., Redon, C. E., Nakamura, A. J., Baird, B. J., Sedelnikova, O. A., & Bonner, W. M. (2009). H2AX: Functional roles and potential applications. *Chromosoma*, *118*(6), 683–692. <https://doi.org/10.1007/s00412-009-0234-4>
78. Nabetani, A., Yokoyama, O., & Ishikawa, F. (2004). Localization of hRad9, hHus1, hRad1, and hRad17 and caffeine-sensitive DNA replication at the alternative lengthening of telomeres-associated promyelocytic leukemia body. *The Journal of Biological Chemistry*, *279*(24), 25849–25857. <https://doi.org/10.1074/jbc.M312652200>
79. Potts, P. R., & Yu, H. (2007). The SMC5/6 complex maintains telomere length in ALT cancer cells through SUMOylation of telomere-binding proteins. *Nature Structural & Molecular Biology*, *14*(7), 581–590. <https://doi.org/10.1038/nsmb1259>
80. Zhang, J.-M., Genois, M.-M., Ouyang, J., Lan, L., & Zou, L. (2021). Alternative lengthening of telomeres is a self-perpetuating process in ALT-associated PML bodies. *Molecular Cell*, *81*(5), 1027-1042.e4. <https://doi.org/10.1016/j.molcel.2020.12.030>
81. Henson, J. D., Cao, Y., Huschtscha, L. I., Chang, A. C., Au, A. Y. M., Pickett, H. A., & Reddel, R. R. (2009). DNA C-circles are specific and quantifiable markers of alternative-lengthening-of-telomeres activity. *Nature Biotechnology*, *27*(12), 1181–1185. <https://doi.org/10.1038/nbt.1587>
82. Henson, J. D., Lau, L. M., Koch, S., Martin La Rotta, N., Dagg, R. A., & Reddel, R. R. (2017). The C-Circle Assay for alternative-lengthening-of-telomeres activity. *Methods*, *114*, 74–84. <https://doi.org/10.1016/j.ymeth.2016.08.016>
83. Chen, Y.-Y., Dagg, R., Zhang, Y., Lee, J. H. Y., Lu, R., Martin La Rotta, N., Sampl, S., Korkut-Demirbaş, M., Holzmann, K., Lau, L. M. S., Reddel, R. R., & Henson, J. D. (2021). The C-Circle Biomarker Is Secreted by Alternative-Lengthening-of-Telomeres Positive Cancer Cells inside Exosomes and Provides a Blood-Based Diagnostic for ALT Activity. *Cancers*, *13*(21), Article 21. <https://doi.org/10.3390/cancers13215369>

84. Tokutake, Y., Matsumoto, T., Watanabe, T., Maeda, S., Tahara, H., Sakamoto, S., Niida, H., Sugimoto, M., Ide, T., & Furuichi, Y. (1998). Extra-Chromosomal Telomere Repeat DNA in Telomerase-Negative Immortalized Cell Lines. *Biochemical and Biophysical Research Communications*, 247(3), 765–772. <https://doi.org/10.1006/bbrc.1998.8876>
85. Ogino, H., Nakabayashi, K., Suzuki, M., Takahashi, E., Fujii, M., Suzuki, T., & Ayusawa, D. (1998). Release of Telomeric DNA from Chromosomes in Immortal Human Cells Lacking Telomerase Activity. *Biochemical and Biophysical Research Communications*, 248(2), 223–227. <https://doi.org/10.1006/bbrc.1998.8875>
86. Cesare, A. J., & Griffith, J. D. (2004). Telomeric DNA in ALT Cells Is Characterized by Free Telomeric Circles and Heterogeneous t-Loops. *Molecular and Cellular Biology*, 24(22), 9948–9957. <https://doi.org/10.1128/MCB.24.22.9948-9957.2004>
87. Nabetani, A., & Ishikawa, F. (2009). Unusual Telomeric DNAs in Human Telomerase-Negative Immortalized Cells. *Molecular and Cellular Biology*, 29(3), 703–713. <https://doi.org/10.1128/MCB.00603-08>
88. Murnane, J. P., Sabatier, L., Marder, B. A., & Morgan, W. F. (1994). Telomere dynamics in an immortal human cell line. *The EMBO Journal*, 13(20), 4953–4962. <https://doi.org/10.1002/j.1460-2075.1994.tb06822.x>
89. Dunham, M. A., Neumann, A. A., Fasching, C. L., & Reddel, R. R. (2000). Telomere maintenance by recombination in human cells. *Nature Genetics*, 26(4), Article 4. <https://doi.org/10.1038/82586>
90. Londoño-Vallejo, J. A., Der-Sarkissian, H., Cazes, L., Bacchetti, S., & Reddel, R. R. (2004). Alternative Lengthening of Telomeres Is Characterized by High Rates of Telomeric Exchange. *Cancer Research*, 64(7), 2324–2327. <https://doi.org/10.1158/0008-5472.CAN-03-4035>
91. Lovejoy, C. A., Li, W., Reisenweber, S., Thongthip, S., Bruno, J., Lange, T. de, De, S., Petrini, J. H. J., Sung, P. A., Jasin, M., Rosenbluh, J., Zwang, Y., Weir, B. A., Hatton, C., Ivanova, E., Macconail, L., Hanna, M., Hahn, W. C., Lue, N. F., ... Consortium, for the A. S. C. (2012). Loss of ATRX, Genome Instability, and an Altered DNA Damage Response Are Hallmarks of the Alternative Lengthening of Telomeres Pathway. *PLOS Genetics*, 8(7), e1002772. <https://doi.org/10.1371/journal.pgen.1002772>
92. Schwartzenuber, J., Korshunov, A., Liu, X.-Y., Jones, D. T. W., Pfaff, E., Jacob, K., Sturm, D., Fontebasso, A. M., Quang, D.-A. K., Tönjes, M., Hovestadt, V., Albrecht, S., Kool, M., Nantel, A., Konermann, C., Lindroth, A., Jäger, N.,

- Rausch, T., Ryzhova, M., ... Jabado, N. (2012). Driver mutations in histone H3.3 and chromatin remodelling genes in paediatric glioblastoma. *Nature*, *482*(7384), Article 7384. <https://doi.org/10.1038/nature10833>
93. Napier, C. E., Huschtscha, L. I., Harvey, A., Bower, K., Noble, J. R., Hendrickson, E. A., & Reddel, R. R. (2015). ATRX represses alternative lengthening of telomeres. *Oncotarget*, *6*(18), 16543–16558. <https://doi.org/10.18632/oncotarget.3846>
94. Lewis, P. W., Elsaesser, S. J., Noh, K.-M., Stadler, S. C., & Allis, C. D. (2010). Daxx is an H3.3-specific histone chaperone and cooperates with ATRX in replication-independent chromatin assembly at telomeres. *Proceedings of the National Academy of Sciences*, *107*(32), 14075–14080. <https://doi.org/10.1073/pnas.1008850107>
95. Elsaesser, S. J., Goldberg, A. D., & Allis, C. D. (2010). New functions for an old variant: No substitute for histone H3.3. *Current Opinion in Genetics & Development*, *20*(2), 110–117. <https://doi.org/10.1016/j.gde.2010.01.003>
96. Goldberg, A. D., Banaszynski, L. A., Noh, K.-M., Lewis, P. W., Elsaesser, S. J., Stadler, S., Dewell, S., Law, M., Guo, X., Li, X., Wen, D., Chapgier, A., DeKever, R. C., Miller, J. C., Lee, Y.-L., Boydston, E. A., Holmes, M. C., Gregory, P. D., Grealley, J. M., ... Allis, C. D. (2010). Distinct Factors Control Histone Variant H3.3 Localization at Specific Genomic Regions. *Cell*, *140*(5), 678–691. <https://doi.org/10.1016/j.cell.2010.01.003>
97. Hoang, S. M., Kaminski, N., Bhargava, R., Barroso-González, J., Lynskey, M. L., García-Expósito, L., Roncaioli, J. L., Wondisford, A. R., Wallace, C. T., Watkins, S. C., James, D. I., Waddell, I. D., Ogilvie, D., Smith, K. M., da Veiga Leprevost, F., Mellacharevu, D., Nesvizhskii, A. I., Li, J., Ray-Gallet, D., ... O'Sullivan, R. J. (2020). Regulation of ALT-associated homology-directed repair by polyADP-ribosylation. *Nature Structural & Molecular Biology*, *27*(12), Article 12. <https://doi.org/10.1038/s41594-020-0512-7>
98. Guervilly, J.-H., & Gaillard, P. H. (2018). SLX4: Multitasking to maintain genome stability. *Critical Reviews in Biochemistry and Molecular Biology*, *53*(5), 475–514. <https://doi.org/10.1080/10409238.2018.1488803>
99. Bussen, W., Raynard, S., Busygina, V., Singh, A. K., & Sung, P. (2007). Holliday Junction Processing Activity of the BLM-Topo III $\alpha$ -BLAP75 Complex. *Journal of Biological Chemistry*, *282*(43), 31484–31492. <https://doi.org/10.1074/jbc.M706116200>
100. Panier, S., Maric, M., Hewitt, G., Mason-Osann, E., Gali, H., Dai, A., Labadorf, A., Guervilly, J.-H., Ruis, P., Segura-Bayona, S., Belan, O., Marzec, P., Gaillard, P.-

- H. L., Flynn, R. L., & Boulton, S. J. (2019). SLX4IP Antagonizes Promiscuous BLM Activity during ALT Maintenance. *Molecular Cell*, 76(1), 27-43.e11. <https://doi.org/10.1016/j.molcel.2019.07.010>
101. de Nonneville, A., Salas, S., Bertucci, F., Sobinoff, A. P., Adélaïde, J., Guille, A., Finetti, P., Noble, J. R., Churikov, D., Chaffanet, M., Lavit, E., Pickett, H. A., Bouvier, C., Birnbaum, D., Reddel, R. R., & Géli, V. (2022). TOP3A amplification and ATRX inactivation are mutually exclusive events in pediatric osteosarcomas using ALT. *EMBO Molecular Medicine*, e15859. <https://doi.org/10.15252/emmm.202215859>
102. Diplas, B. H., He, X., Brosnan-Cashman, J. A., Liu, H., Chen, L. H., Wang, Z., Moure, C. J., Killela, P. J., Loriaux, D. B., Lipp, E. S., Greer, P. K., Yang, R., Rizzo, A. J., Rodriguez, F. J., Friedman, A. H., Friedman, H. S., Wang, S., He, Y., McLendon, R. E., ... Yan, H. (2018). The genomic landscape of TERT promoter wildtype-IDH wildtype glioblastoma. *Nature Communications*, 9(1), Article 1. <https://doi.org/10.1038/s41467-018-04448-6>
103. Mason-Osann, E., Dai, A., Floro, J., Lock, Y. J., Reiss, M., Gali, H., Matschulat, A., Labadorf, A., Flynn, R. L., Mason-Osann, E., Dai, A., Floro, J., Lock, Y. J., Reiss, M., Gali, H., Matschulat, A., Labadorf, A., & Flynn, R. L. (2018). Identification of a novel gene fusion in ALT positive osteosarcoma. *Oncotarget*, 9(67), 32868–32880. <https://doi.org/10.18632/oncotarget.26029>
104. Brosnan-Cashman, J. A., Davis, C. M., Diplas, B. H., Meeker, A. K., Rodriguez, F. J., & Heaphy, C. M. (2021). SMARCAL1 loss and alternative lengthening of telomeres (ALT) are enriched in giant cell glioblastoma. *Modern Pathology*, 34(10), Article 10. <https://doi.org/10.1038/s41379-021-00841-7>
105. Yuan, J., Ghosal, G., & Chen, J. (2009). The annealing helicase HARP protects stalled replication forks. *Genes & Development*, 23(20), 2394–2399. <https://doi.org/10.1101/gad.1836409>
106. Bansbach, C. E., Bétous, R., Lovejoy, C. A., Glick, G. G., & Cortez, D. (2009). The annealing helicase SMARCAL1 maintains genome integrity at stalled replication forks. *Genes & Development*, 23(20), 2405–2414. <https://doi.org/10.1101/gad.1839909>
107. Postow, L., Woo, E. M., Chait, B. T., & Funabiki, H. (2009). Identification of SMARCAL1 as a Component of the DNA Damage Response. *Journal of Biological Chemistry*, 284(51), 35951–35961. <https://doi.org/10.1074/jbc.M109.048330>

108. Ghosal, G., Yuan, J., & Chen, J. (2011). The HARP domain dictates the annealing helicase activity of HARP/SMARCAL1. *EMBO Reports*, *12*(6), 574–580. <https://doi.org/10.1038/embor.2011.74>
109. Yusufzai, T., & Kadonaga, J. T. (2008). HARP Is an ATP-Driven Annealing Helicase. *Science*, *322*(5902), 748–750. <https://doi.org/10.1126/science.1161233>
110. Poole, L. A., Zhao, R., Glick, G. G., Lovejoy, C. A., Eischen, C. M., & Cortez, D. (2015). SMARCAL1 maintains telomere integrity during DNA replication. *Proceedings of the National Academy of Sciences*, *112*(48), 14864–14869. <https://doi.org/10.1073/pnas.1510750112>
111. Ciccia, A., Bredemeyer, A. L., Sowa, M. E., Terret, M.-E., Jallepalli, P. V., Harper, J. W., & Elledge, S. J. (2009). The SIOD disorder protein SMARCAL1 is an RPA-interacting protein involved in replication fork restart. *Genes & Development*, *23*(20), 2415–2425. <https://doi.org/10.1101/gad.1832309>
112. Dyer, M. A., Qadeer, Z. A., Valle-Garcia, D., & Bernstein, E. (2017). ATRX and DAXX: Mechanisms and Mutations. *Cold Spring Harbor Perspectives in Medicine*, *7*(3), a026567. <https://doi.org/10.1101/cshperspect.a026567>
113. Hakin-Smith, V., Jellinek, D., Levy, D., Carroll, T., Teo, M., Timperley, W., McKay, M., Reddel, R., & Royds, J. (2003). Alternative lengthening of telomeres and survival in patients with glioblastoma multiforme. *The Lancet*, *361*(9360), 836–838. [https://doi.org/10.1016/S0140-6736\(03\)12681-5](https://doi.org/10.1016/S0140-6736(03)12681-5)
114. McDonald, K. L., McDonnell, J., Muntoni, A., Henson, J. D., Hegi, M. E., von Deimling, A., Wheeler, H. R., Cook, R. J., Biggs, M. T., Little, N. S., Robinson, B. G., Reddel, R. R., & Royds, J. A. (2010). Presence of Alternative Lengthening of Telomeres Mechanism in Patients With Glioblastoma Identifies a Less Aggressive Tumor Type With Longer Survival. *Journal of Neuropathology & Experimental Neurology*, *69*(7), 729–736. <https://doi.org/10.1097/NEN.0b013e3181e576cf>
115. Lawlor, R. T., Veronese, N., Pea, A., Nottegar, A., Smith, L., Pilati, C., Demurtas, J., Fassan, M., Cheng, L., & Luchini, C. (2019). Alternative lengthening of telomeres (ALT) influences survival in soft tissue sarcomas: A systematic review with meta-analysis. *BMC Cancer*, *19*(1), 232. <https://doi.org/10.1186/s12885-019-5424-8>
116. Sung, J.-Y., Lim, H.-W., Joung, J.-G., & Park, W.-Y. (2020). Pan-Cancer Analysis of Alternative Lengthening of Telomere Activity. *Cancers*, *12*(8), Article 8. <https://doi.org/10.3390/cancers12082207>

117. Hackeng, W. M., Brosens, L. A. A., Kim, J. Y., O'Sullivan, R., Sung, Y.-N., Liu, T.-C., Cao, D., Heayn, M., Brosnan-Cashman, J., An, S., Morsink, F. H. M., Heidsma, C. M., Valk, G. D., Vriens, M. R., Dijkum, E. N. van, Offerhaus, G. J. A., Dreijerink, K. M. A., Zeh, H., Zureikat, A. H., ... Singhi, A. D. (2022). Non-functional pancreatic neuroendocrine tumours: ATRX/DAXX and alternative lengthening of telomeres (ALT) are prognostically independent from ARX/PDX1 expression and tumour size. *Gut*, *71*(5), 961–973. <https://doi.org/10.1136/gutjnl-2020-322595>
118. Udrouiu, I., & Sgura, A. (2020). Alternative Lengthening of Telomeres and Chromatin Status. *Genes*, *11*(1), Article 1. <https://doi.org/10.3390/genes11010045>
119. Cubiles, M. D., Barroso, S., Vaquero-Sedas, M. I., Enguix, A., Aguilera, A., & Vega-Palas, M. A. (2018). Epigenetic features of human telomeres. *Nucleic Acids Research*, *46*(5), 2347–2355. <https://doi.org/10.1093/nar/gky006>
120. Gauchier, M., Kan, S., Barral, A., Sauzet, S., Agirre, E., Bonnell, E., Saksouk, N., Barth, T. K., Ide, S., Urbach, S., Wellinger, R. J., Luco, R. F., Imhof, A., & Déjardin, J. (2019). SETDB1-dependent heterochromatin stimulates alternative lengthening of telomeres. *Science Advances*, *5*(5), eaav3673. <https://doi.org/10.1126/sciadv.aav3673>
121. Udugama, M., M. Chang, F. T., Chan, F. L., Tang, M. C., Pickett, H. A., R. McGhie, J. D., Mayne, L., Collas, P., Mann, J. R., & Wong, L. H. (2015). Histone variant H3.3 provides the heterochromatic H3 lysine 9 tri-methylation mark at telomeres. *Nucleic Acids Research*, *43*(21), 10227–10237. <https://doi.org/10.1093/nar/gkv847>
122. Zeineldin, M., Federico, S., Chen, X., Fan, Y., Xu, B., Stewart, E., Zhou, X., Jeon, J., Griffiths, L., Nguyen, R., Norrie, J., Easton, J., Mulder, H., Yergeau, D., Liu, Y., Wu, J., Van Ryn, C., Naranjo, A., Hogarty, M. D., ... Dyer, M. A. (2020). MYCN amplification and ATRX mutations are incompatible in neuroblastoma. *Nature Communications*, *11*(1), Article 1. <https://doi.org/10.1038/s41467-020-14682-6>
123. Liu, W., Krishnamoorthy, A., Zhao, R., & Cortez, D. (2020). Two replication fork remodeling pathways generate nuclease substrates for distinct fork protection factors. *Science Advances*, *6*(46), eabc3598. <https://doi.org/10.1126/sciadv.abc3598>
124. Rosenfeld, J. A., Wang, Z., Schones, D. E., Zhao, K., DeSalle, R., & Zhang, M. Q. (2009). Determination of enriched histone modifications in non-genic portions of the human genome. *BMC Genomics*, *10*(1), 143. <https://doi.org/10.1186/1471-2164-10-143>

125. O'Sullivan, R. J., Kubicek, S., Schreiber, S. L., & Karlseder, J. (2010). Reduced histone biosynthesis and chromatin changes arising from a damage signal at telomeres. *Nature Structural & Molecular Biology*, *17*(10), Article 10. <https://doi.org/10.1038/nsmb.1897>
126. Arnoult, N., Van Beneden, A., & Decottignies, A. (2012). Telomere length regulates TERRA levels through increased trimethylation of telomeric H3K9 and HP1 $\alpha$ . *Nature Structural & Molecular Biology*, *19*(9), Article 9. <https://doi.org/10.1038/nsmb.2364>
127. Montero, J. J., López-Silanes, I., Megías, D., F. Fraga, M., Castells-García, Á., & Blasco, M. A. (2018). TERRA recruitment of polycomb to telomeres is essential for histone trimethylation marks at telomeric heterochromatin. *Nature Communications*, *9*(1), Article 1. <https://doi.org/10.1038/s41467-018-03916-3>
128. García-Cao, M., O'Sullivan, R., Peters, A. H. F. M., Jenuwein, T., & Blasco, M. A. (2004). Epigenetic regulation of telomere length in mammalian cells by the Suv39h1 and Suv39h2 histone methyltransferases. *Nature Genetics*, *36*(1), Article 1. <https://doi.org/10.1038/ng1278>
129. Blasco, M. A. (2007). The epigenetic regulation of mammalian telomeres. *Nature Reviews Genetics*, *8*(4), Article 4. <https://doi.org/10.1038/nrg2047>
130. Canzio, D., Larson, A., & Narlikar, G. J. (2014). Mechanisms of functional promiscuity by HP1 proteins. *Trends in Cell Biology*, *24*(6), 377–386. <https://doi.org/10.1016/j.tcb.2014.01.002>
131. Lachner, M., O'Carroll, D., Rea, S., Mechtler, K., & Jenuwein, T. (2001). Methylation of histone H3 lysine 9 creates a binding site for HP1 proteins. *Nature*, *410*(6824), Article 6824. <https://doi.org/10.1038/35065132>
132. Nielsen, P. R., Nietlispach, D., Mott, H. R., Callaghan, J., Bannister, A., Kouzarides, T., Murzin, A. G., Murzina, N. V., & Laue, E. D. (2002). Structure of the HP1 chromodomain bound to histone H3 methylated at lysine 9. *Nature*, *416*(6876), Article 6876. <https://doi.org/10.1038/nature722>
133. Smothers, J. F., & Henikoff, S. (2000). The HP1 chromo shadow domain binds a consensus peptide pentamer. *Current Biology*, *10*(1), 27–30. [https://doi.org/10.1016/S0960-9822\(99\)00260-2](https://doi.org/10.1016/S0960-9822(99)00260-2)
134. Canudas, S., Houghtaling, B. R., Bhanot, M., Sasa, G., Savage, S. A., Bertuch, A. A., & Smith, S. (2011). A role for heterochromatin protein 1 $\gamma$  at human telomeres. *Genes & Development*, *25*(17), 1807–1819. <https://doi.org/10.1101/gad.17325211>

135. Maeda, R., & Tachibana, M. (2022). HP1 maintains protein stability of H3K9 methyltransferases and demethylases. *EMBO Reports*, *23*(4), e53581. <https://doi.org/10.15252/embr.202153581>
136. Mason, A. C., Rambo, R. P., Greer, B., Pritchett, M., Tainer, J. A., Cortez, D., & Eichman, B. F. (2014). A structure-specific nucleic acid-binding domain conserved among DNA repair proteins. *Proceedings of the National Academy of Sciences*, *111*(21), 7618–7623. <https://doi.org/10.1073/pnas.1324143111>
137. Lavigne, M., Eskeland, R., Azebi, S., Saint-André, V., Jang, S. M., Batsché, E., Fan, H.-Y., Kingston, R. E., Imhof, A., & Muchardt, C. (2009). Interaction of HP1 and Brg1/Brm with the Globular Domain of Histone H3 Is Required for HP1-Mediated Repression. *PLOS Genetics*, *5*(12), e1000769. <https://doi.org/10.1371/journal.pgen.1000769>
138. Yang, B., Xu, X., Russell, L., Sullenberger, M. T., Yanowitz, J. L., & Maine, E. M. (2019). A DNA repair protein and histone methyltransferase interact to promote genome stability in the *Caenorhabditis elegans* germ line. *PLOS Genetics*, *15*(2), e1007992. <https://doi.org/10.1371/journal.pgen.1007992>
139. Mateescu, B., Bourachot, B., Rachez, C., Ogryzko, V., & Muchardt, C. (2008). Regulation of an inducible promoter by an HP1 $\beta$ –HP1 $\gamma$  switch. *EMBO Reports*, *9*(3), 267–272. <https://doi.org/10.1038/embor.2008.1>
140. Halder, S., Ranjha, L., Taglialatela, A., Ciccia, A., & Cejka, P. (2022). Strand annealing and motor driven activities of SMARCAL1 and ZRANB3 are stimulated by RAD51 and the paralog complex. *Nucleic Acids Research*, *50*(14), 8008–8022. <https://doi.org/10.1093/nar/gkac583>
141. He, W., Zhang, L., Villarreal, O. D., Fu, R., Bedford, E., Dou, J., Patel, A. Y., Bedford, M. T., Shi, X., Chen, T., Bartholomew, B., & Xu, H. (2019). De novo identification of essential protein domains from CRISPR-Cas9 tiling-sgRNA knockout screens. *Nature Communications*, *10*(1), Article 1. <https://doi.org/10.1038/s41467-019-12489-8>

**CURRICULUM VITAE**

